Overarching Responses to the Reviewers

Format: The reviewer's comments are quoted in italic

Line number in the response refers to the revised manuscript with tracked changes

Quotation in red color stands for revised/added text in the revised manuscript

We thank our reviewers for the helpful comments they took the time to provide us with. We would also like to thank the three reviewers and the leading editor for their patience on our responses. Earlier this year, my former student (Flor, who is now a PhD candidate at UCLA) and I myself each experienced unexpected difficulties and stress with our close family member's health. We each had to take the main responsibility for our family care for a while, which led to an unprecedented disruption to both of our regular work. I also invited my current graduate student, Ching An Yang (our new third coauthor), for her help with our preparation of the new figures since Ching had previous experience with the NSF SOCRATES data in her paper Yang et al. (2021) published in JGR-Atmosphere.

Below is a summary of the main revisions that we conducted, followed by our individual response to each reviewer. Overall, we revised almost all original figures and table 1, added new Figure 4, new supplemental Figures S1 – S10 and Table S1.

1. We have done a thorough data quality control on multiple instruments, including measurements of relative humidity, vertical velocity, and several cloud probes, 2DS, CDP and 2DC. We elaborate our quality control results in our response below to reviewer 2.

2. We conducted analysis of two new remote sensing instruments (i.e., HIAPER Cloud Radar and High Spectral Resolution Lidar) onboard the Gulfstream-V aircraft during the SOCRATES campaign, in order to address the concerns of precipitation by reviewer 3 and as a possible approach to examine cloud vertical layers in a comment raised by reviewer 1.

3. We expanded the possible pathways for cloud evolution as recommended by reviewer 2, and added more context on how the transition phases in this work are related to the previous studies.

Response to comments from Reviewer 1

Review of "The Transition from Supercooled Liquid Water to Ice Crystals in Mixed-phase Clouds based on Airborne In-situ Observations", by Maciel and Diao.

This is an interesting and I'd say novel study that characterizes the degree of glaciation of supercooled clouds in the Southern Ocean, using data from the SOCRATES field program. They use a combination of "bulk" data from the 2DS and CDP probes, augmented with the King liquid water content and Rosemont Icing Probes for phase discrimination. The methodology is based on Yang et al. (2021), which is based on D'Alessandro et al. (2019). A second method uses the 2DS images and a machine learning tool to identify individual images of liquid and ice particles. The methodology and some of the results bear a striking similarity to the Yang et al. (2021) article. This includes the relationship of the phase partitioning to the aerosol concentration. Some mention of the results of that study should be given and how the techniques and results differ.

We thank the reviewer for the helpful comments and below is our response to each of them.

Regarding the differences with Yang et al. (2021) paper, the main differences are that this work separates the transition phases of clouds instead of analyzing all clouds together, and this work compares different methods to define liquid, mixed and ice phase, including using the microphysical properties of hydrometeor mass concentrations or number concentrations, and the macrophysical properties of the

spatial fraction of ice-containing segments. Below are two examples where we distinguish this current work from that of Yang et al. (2021).

One example is that we modified the cloud phase identification for the 2DS probe compared with Yang et al. (2021): "… The second modification is about the treatment of large particles identified as liquid droplets. The previous method restricts particles with maximum dimensions (D_{max}) > 312.5 μm as ice particles, while those with D_{max} between 112.5 and 312.5 μm can be either liquid or ice depending on the standard deviation of particle sizes measured by 2DS in that second. In this work, we restrict particles with D_{max} > 212.5 μm to be ice particles, reducing the number of large particles being categorized as liquid droplets."

Another example is about the aerosol indirect effect analysis: "Stronger positive correlations between IWC and $N_{>500}$ compared with $N_{>100}$ are also shown in the previous work by Yang et al. (2021), although that study did not differentiate the transition phase of clouds nor examine aerosol indirect effects in relation to cloud macrophysical properties, i.e., the spatial expansion of ice-containing cloud segments."

The partitioning of the data into liquid only, mostly liquid, mostly ice and all ice phases is interesting, and relating it to the macrophysical properties of the cloud layer (ice content, relative humidity with respect to water and ice, and vertical velocity is interesting. Likewise, the ice fraction partitioning is rather interesting.

I tried to think of the factors that determine the glaciation of a stratiform cloud layer. First, in stratiform ice cloud layers, typically liquid water regions, the stronger vertical motions, and ice nucleation mostly occur at cloud top. Below cloud top and depending on the vertical velocity which is responsible for the degree of ice supersaturation or subsaturation, can contain a growth or sublimation layer. The measurements you report on do not account for where vertically within the cloud layer relative to cloud top the aircraft penetrations were made. Thus, you may be sampling in a subsident or upward moving parcel of air. Perhaps your measurements at temperatures below -15^{0}C are near cloud top, and those at the warmer temperatures in the middle or lower parts of the cloud layers. The relationship of the relative humidity to turbulence might be a manifestation of where in the cloud layer the sampling is done, and whether generating cells were penetrated. You do mention that the aircraft observations only captures the 1-D structure of a cloud segment, while cloud layers above and below the aircraft flight track may show a different ice spatial ratio on a 2-D or 3-D view. Nonetheless, I think a weakness of the study is that there is no partitioning of where in the cloud layer the measurements are made. (Note that it's unlikely that the vertical motions measured by the aircraft system are sufficiently accurate to determine what zone the measurements are made in, unless generating cells are penetrated).

We thank the reviewer for this helpful comment. We agree that identifying the location of the aircraft in-situ sampling relative to the cloud vertical layer would be helpful. We tried the approach of analyzing the two airborne remote sensing instruments onboard – HIAPER Cloud Radar (HCR) and High Spectral Resolution Lidar (HSRL), which provide some profiling either above or below the aircraft flight track. But we ran into issues that the remote sensing data are only pointed toward one direction at a given time, so we can only inspect either above or below the aircraft for what the cloud layers were like. Also, the remote sensing instruments cannot measure in close proximity to the aircraft, which leave an area without remote sensing data surrounding the flight track. Since trying this approach does not provide a straightforward answer, we also tried looking into the field catalogue for possible identification of cloud top, middle, or base sampling. We found that only a few cloud segments have been identified with clear sampling strategies, which would severely affect the sample size that we can utilize. Thus, we decided to address this comment by conducting analysis on regions with different magnitudes of liquid and ice water content (LWC and IWC), and relative humidity with respect to ice (RH_i), since these values typically vary with vertical levels within a cloud as the reviewer mentioned.

Different ranges of LWC, IWC and RH_i are used in the identifications of transition phases in **supplemental Figure S2 - S4**, respectively (shown below), which show small variations in the number of samples of four transition phases. In addition, we contrasted the differences between using all RHi values from the entire in-cloud layer and using only the higher RHi values (RH_i > 80%) that potentially represent the higher levels within a cloud. We found that the differences between them are very small for several key analyses in this work, shown in **supplemental material Figures S7 – S9**, which are comparable with Figures 7, 8 and 9, respectively. Below we put these analyses side-by-side to illustrate the small differences between them. We discussed these additional tests and added suggestions for future field campaigns.

We added discussion in section 3.1: "Since the 1-D aircraft sampling can be at any vertical level relative to a cloud layer, we further examine the impacts of restricting the analysis to different ranges of LWC, IWC, and RHi values (supplementary Figures S2 – S4). Previous studies such as Wang et al. (2012) and D'Alessandro et al. (2023) have shown that cloud top usually contains higher LWC than cloud base, while IWC increases from the cloud top to cloud base. D'Alessandro et al. (2019) also showed that in-cloud samples with higher liquid mass fraction have higher RH values closer to liquid saturation. By using different ranges of LWC, IWC and RHi as proxies for vertical levels within cloud layers, we found that the number of samples of the four transition phases are relatively similar unless very high LWC or IWC are used (> 0.1 g m^{-3})."

We also added comments in section 4: "Future investigation that compares 1-D aircraft sampling with 2-D remote sensing observations and 3-D model simulations is recommended to further examine the quasi-Lagrangian evolution of mixed-phase clouds."

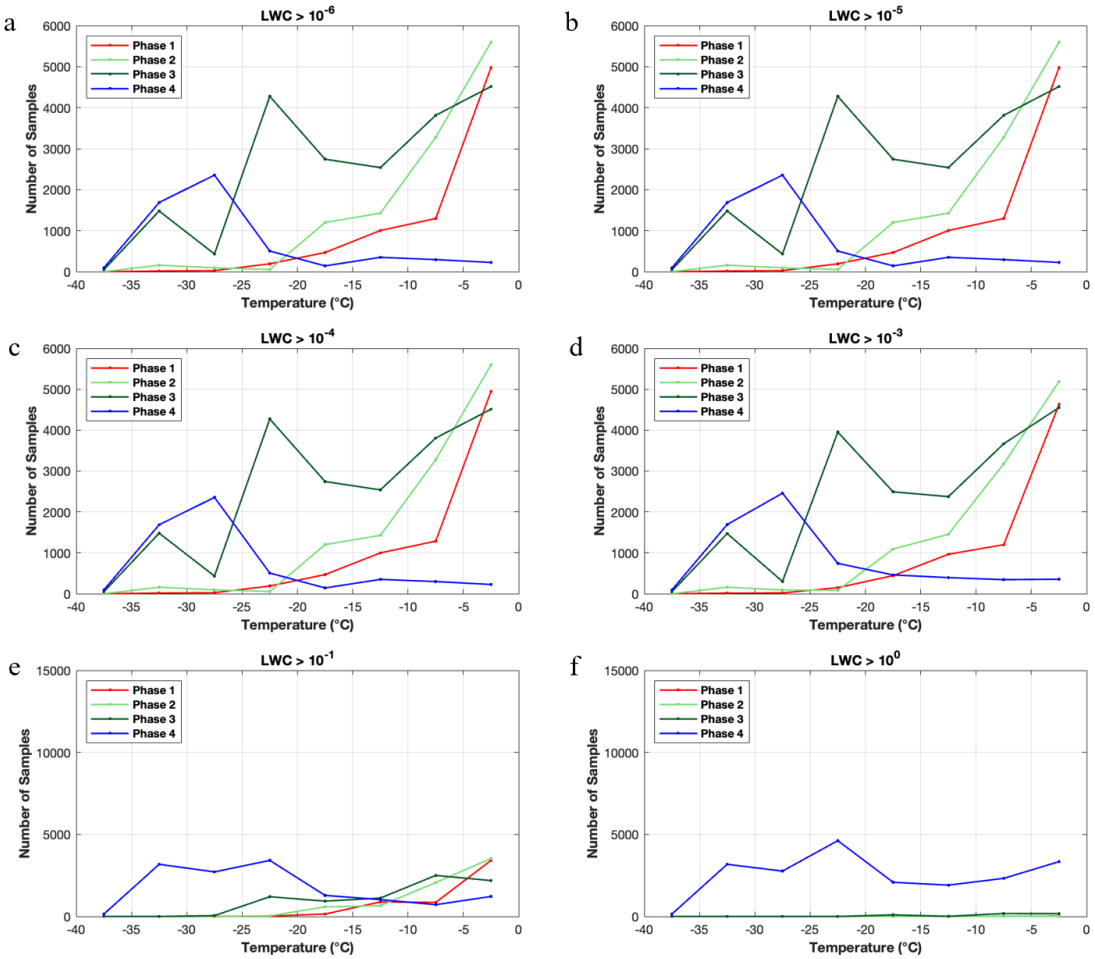

Figure S2. Similar to Figure 3 a, number of samples for four transition phases but using different liquid water content (LWC) values (unit: g m^{-3}) as the threshold for defining in-cloud conditions.

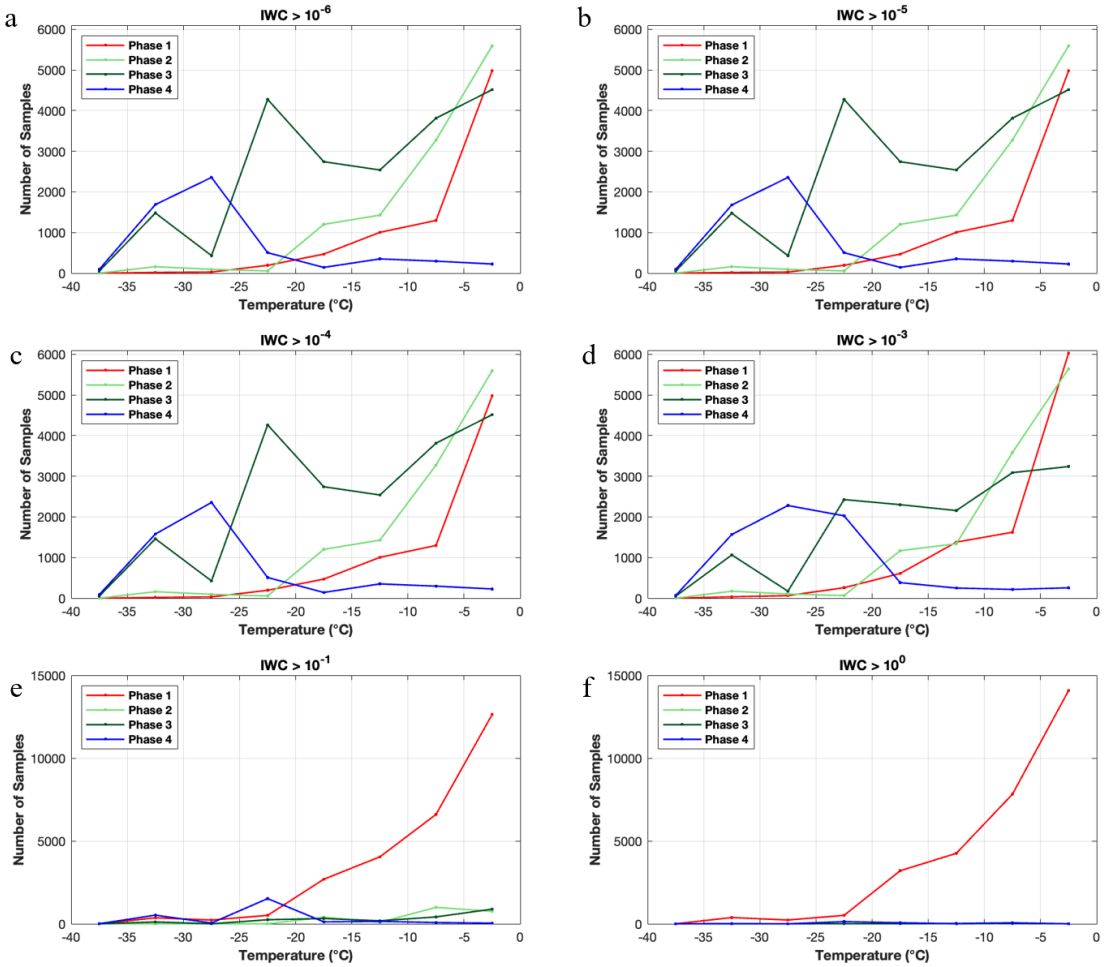

Figure S3. Similar to Figure 3 a, number of samples for four transition phases but using different ice water content (IWC) values (unit: g m^{-3}) as the threshold for defining in-cloud conditions.

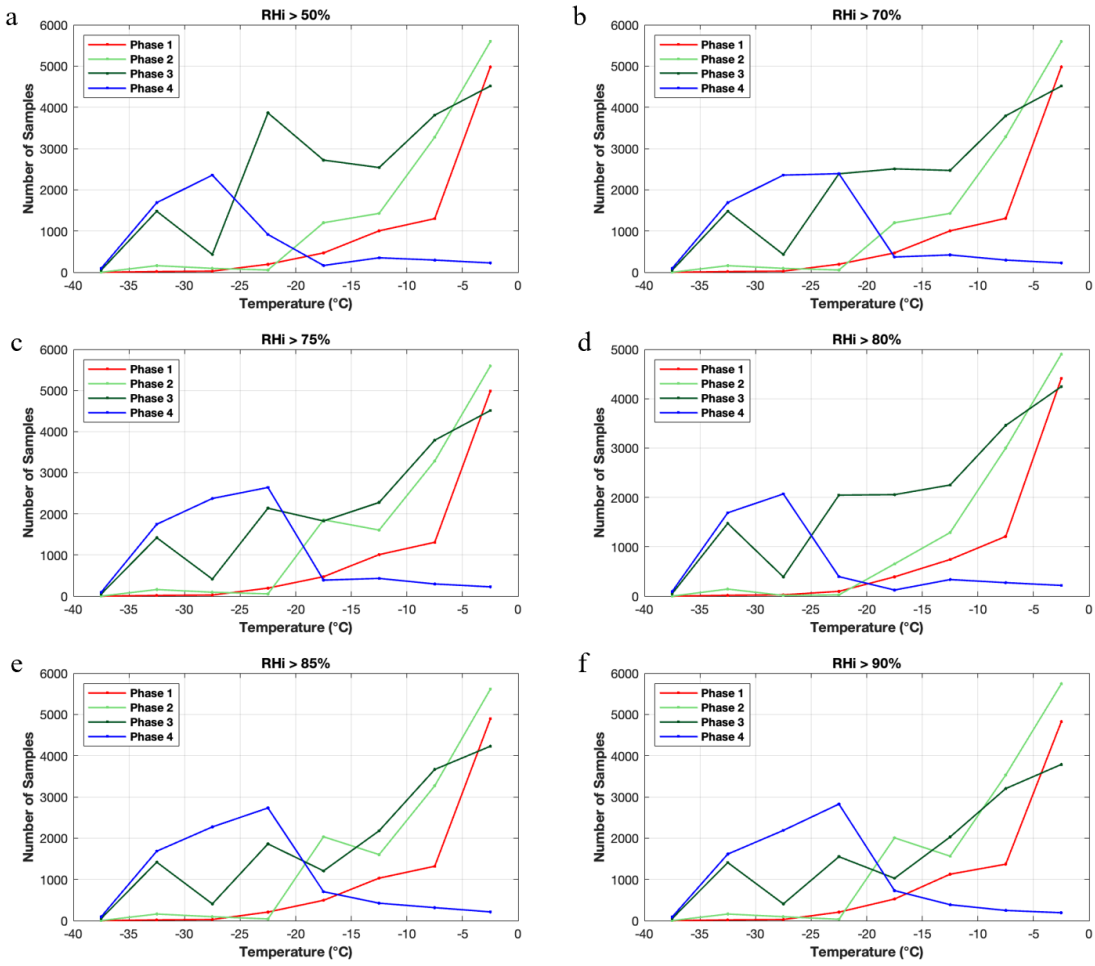

Figure S4. Similar to Figure 3 a, number of samples for four transition phases but using different ranges of relative humidity with respect to ice (RH_i) for analysis of in-cloud conditions.

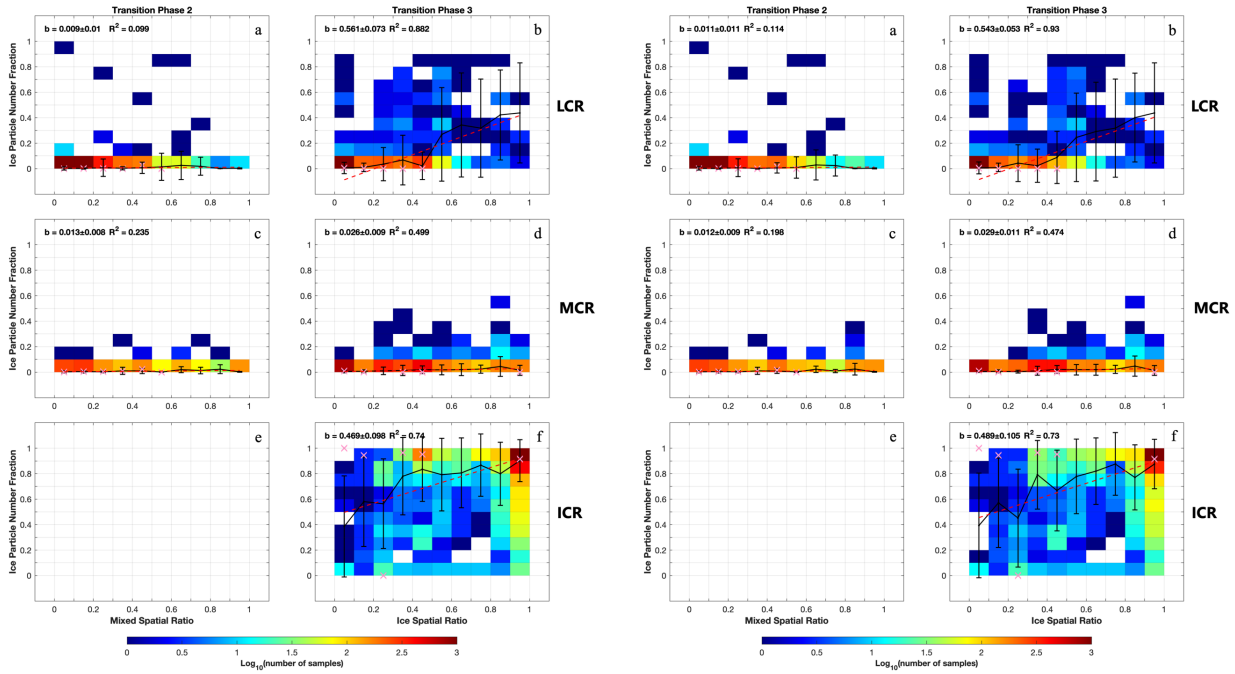

Figure R1-1. Side-by-side comparisons of using all RH_i data (left) versus using only high RH_i (>80%) (right). The figure on the left is Figure 7, on the right is Figure S7.

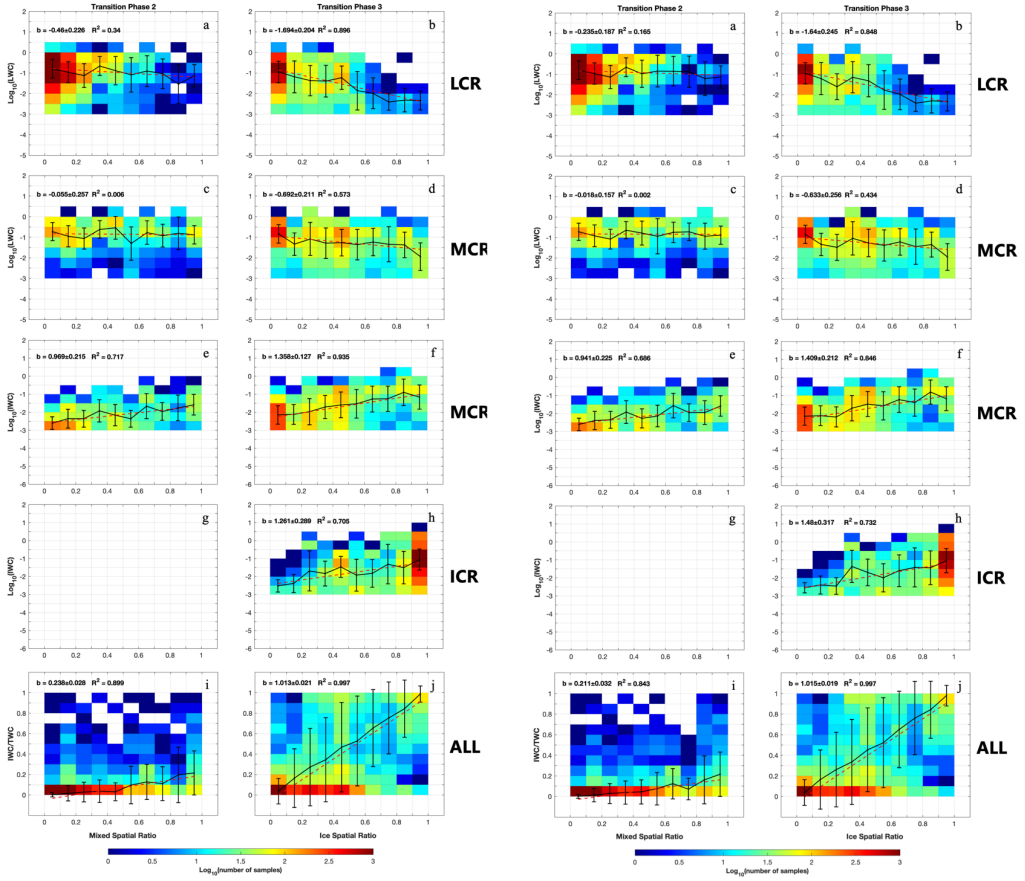

Figure R1-2. Side-by-side comparisons of using all RH_i data (left) versus using only high RH_i (>80%) (right). The figure on the left is Figure 8, on the right is Figure S8.

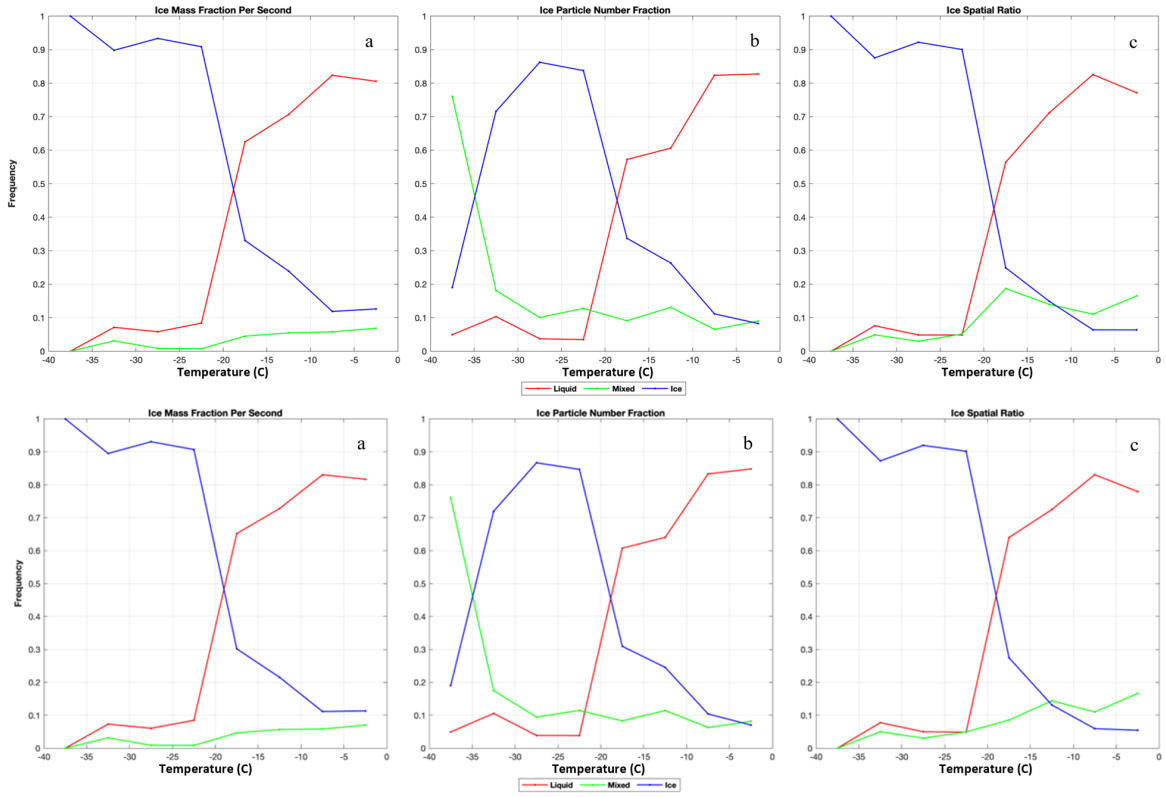

Figure R1-3. Side-by-side comparisons of using all RH_i data (top) versus using only high RH_f (>80%) (bottom). The figure on the top is Figure 9, on the bottom is Figure S9.

Figure 10, which shows the distributions of RHi, RHliq, vertical velocity and standard deviation of vertical velocity which be presented before Figure 3 as it provides a context for how the various transition regions relate to the large-scale properties of the cloud layer. What is shows is that transition region 4 is subsaturated. This why there is no liquid water in that region, not a stage of development of the ice cloud. It also shows up in the PSDs-transition region 4 has fewer ice particles and smaller maximum ice particle sizes than transition region 3. These might be the trails of generating cells, where the growth is aloft and sublimation lower down in the cloud layer.

We moved the original Figures 10 and 11 forward and combined them into the **new Figure 5**. We decided to show Figure 3 first since it provides the number of samples for each phase. We also added new **Figure 4** (shown below) to illustrate the full distribution of RH_i and standard deviation of vertical velocity (σ_w) for each phase. Please note that the RH_i shown in the original Figures 10 and 11 only represents the mean value in each bin. When examining the entire distribution of RH_i, all phases have RH_i being ice supersaturated, saturated and subsaturated. For example, phase 4 has ice supersaturation as well. This is consistent with what reviewer 2 pointed out that another possible pathway of the cloud evolution is that phase 4 pure ice segments can turn into phase 2 with coexisting liquid and ice. We added discussion on this part in section 2.2: "The third pathway of mixed-phase evolution is related to the generation of mixed-phase clouds in a pre-existing ice cloud due to dynamic forcing, which can be presented as ice=>mixed-phase, i.e., phases (4)=>(2), or (4)=>(3)=>(2). Note that the numerical order of phases 1 – 4 does not necessarily represent the evolution direction. For example, phase 4 may either be the final stage in the first classical pathway, whereas in the third pathway, phase 4 is an initial stage."

We agree with reviewer's comments that some of the phase 4 segments could be trails of generating cells, and we added this comment as a new discussion in section 3.3 when describing the particle size distributions (PSDs): "It is possible that some of the phase 4 samples may represent the trails of generating cells, where the growth is aloft, and sublimation is at the lower part of the cloud layer.".

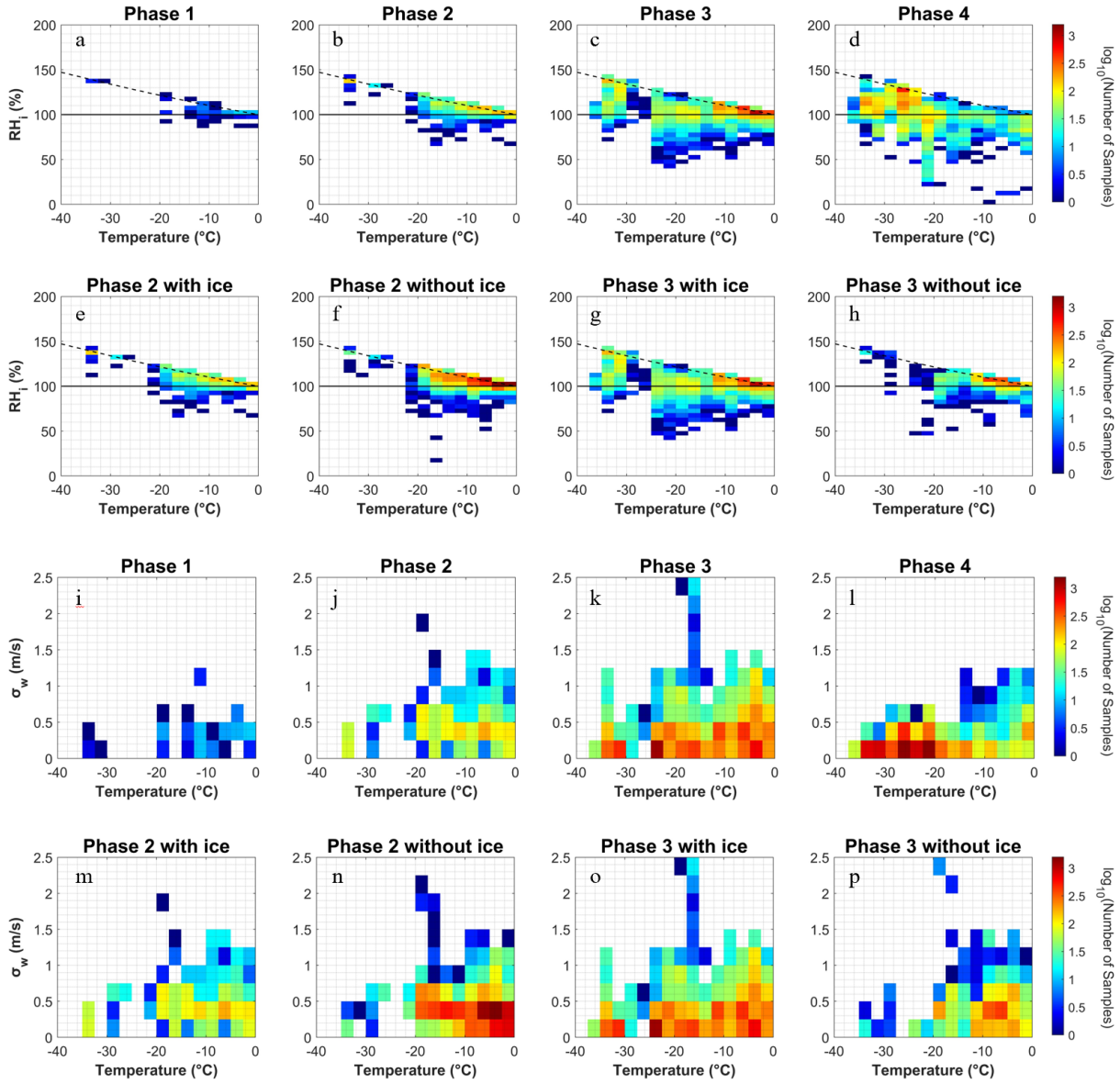

Figure 4. Distributions of (a-h) RH_i and (i-p) σ_w in various transition phases as a function of temperature. Dashed lines in (a) – (h) indicate liquid saturation.

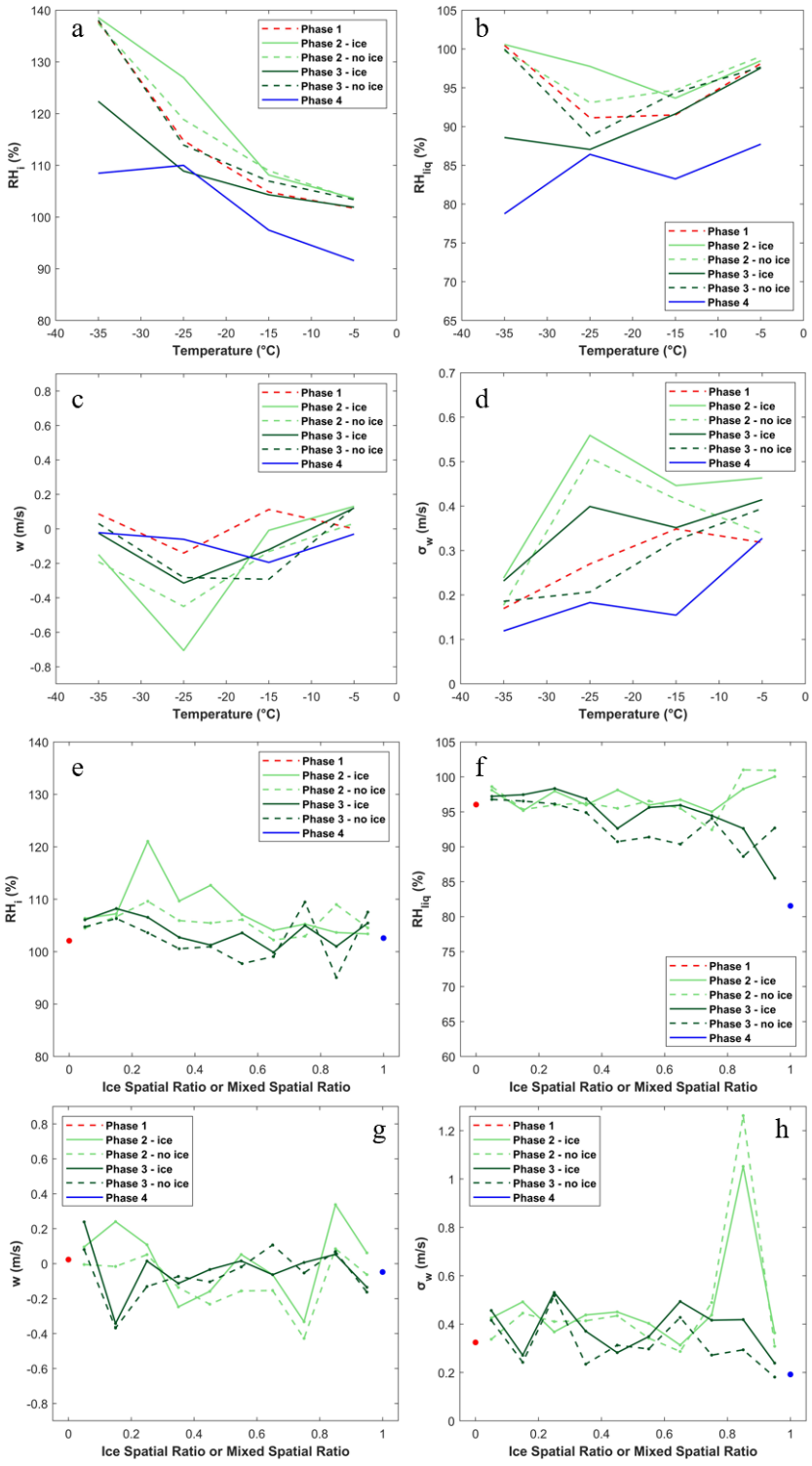

Figure 5. Distributions of (a) RH_i, (b) RH_{liq}, (c) vertical velocity (w) and (d) standard deviation of vertical velocity (σ_w) for various transition phases at different temperatures. (e-h) Similar to (a-d), but in relation to various mixed spatial ratios or ice spatial ratios. Phases 1 and 4 show ice spatial ratio at 0 and 1, respectively, and therefore only a single dot is shown for phases 1 and 4 in (e-h).

Minor comments

Line 6: determines the "ice cloud lifetime"

Revised.

45: resilience to what?

Revised to "The persistent existence of mixed-phase cloud systems".

62: "growing"?

Removed "growing".

66: aerosol

Revised.

97: remove "various"

Removed.

183: I don't think the CDP can reliably differentiate liquid drops from small ice

We thank the reviewer for pointing out this point. We removed the identification of ice by CDP, as also recommended by reviewer 2. In the revised manuscript, only when CDP identifies particles as liquid droplets, these measurements are being used.

186. Phase 4. Perhaps this is due to aggregation reducing the concentration of ice crystals.

Another possibility is that this region is subsaturated. Indeed, the RHi in transition region 4 is subsaturated.

We revised the text to add these new possible explanations: "The decreasing ice crystal concentrations per size bin from phase 3 to phase 4 may be caused by stronger aggregation, sublimation, and/or sedimentation of ice crystals in phase 4, as well as by stronger secondary ice production in phase 3."

190. This is likely due to sublimation in transition region 4.

We added these new possible explanations: "The significant decrease (1 to 4 orders of magnitude) of hydrometeor concentrations per size bin at 20 – 100 μm in phase 4 compared with the other three phases suggests that most supercooled liquid water may have evaporated and transitioned into ice phase through WBF process or riming, instead of the freezing of individual droplets, while the small ice crystals may have sublimated."

Section 3.4. This is similar to the Yang et al. (2021) study.

We added this citation and explained the difference between this study and that previous study: "Stronger positive correlations between IWC and $N_{>500}$ compared with $N_{>100}$ are also shown in the previous work by Yang et al. (2021), although that study did not differentiate the transition phase of clouds nor examine aerosol indirect effects in relation to cloud macrophysical properties, i.e., the spatial expansion of ice-containing cloud segments."

260: Phase 4 has the lowest RHi and RHliq values. In fact, it is subsaturated at most temperatures (Fig. 10a). Consider moving Section 3.5 much earlier, perhaps before charactering the different transition phases. It explains a lot.

We moved the original Figures 10 and 11 forward and they now are combined into one new **Figure 5**. We also added a new **Figure 4** as mentioned above. The section has also been moved forward and it is the new section 3.2.

Response to comments from Reviewer 2

Review of "The Transition from Supercooled Liquid Water to Ice Crystals in Mixed-phase Clouds based on Airborne In-situ Observations" by F.V. Maciel and M. Diao et al. (2022)

Overview

This study is focused on the microphysical characterization of mixed-phase environments and on linking it to the various stages of phase transition. The data explored here was collected in- situ during the SOCRATES field campaigns over the Southern Ocean. Identification of the phase transition stage is based on the assessment of the presence ice, liquid and mixed-phase cloud segments coexisting in the same cloud. Depending on the combination of these three thermodynamic states, the clouds were separated into four categories: (1) liquid, (2) mixed-phase ∧ liquid; (3) mixed-phase ∧ (liquid ∨ ice ∨ (liquid ∧ ice)); (4) ice. Aerosol concentration, in-cloud dynamics and atmospheric state conditions were quantified for each of these four categories. The applied method enabled conclusions regarding the effect of aerosols, atmospheric state and cloud dynamics parameters of the evolution of mixed-phase clouds. This paper is interesting and deserves attention, however, I have concerns about the general approach, data quality and clarity of presentation. I would also recommend a more thorough acknowledgement of past studies on mixed-phase clouds.

Recommendation: I regret to say that, in my opinion, the paper is not suitable for publication in ACP in its present form. I would recommend rewriting the manuscript addressing the comments below and resubmitting the paper.

We thank the reviewer for the helpful comments and below is our response to each of them.

Major comments

Methodology and basic assumptions

1. The proposed method is based on a preconception that, during their lifetime, mixed-phase clouds pass through the stages (1)=>(2)=>(3)=>(4) as described in the paper, i.e., the cloud is initiated as liquid under supercooled conditions; then it experiences nucleation of ice and turns into mixed-phase; after that some section of the mixed-phase cloud glaciates and turns into ice, and in the final stage, the entire cloud is glaciated. The conceptual diagram of this process is shown in Fig.2, and it is used as the basis for the following interpretation of the data. This kind of "classical" evolution of mixed-phase clouds was observed and documented over 35 years ago (e.g., Hobbs and Rangno, 1985). However, besides the classical progression of mixed-phase, there are two other routes of evolution of mixed-phase clouds. The first scenario is when, after nucleation of INPs and turning liquid cloud into mixed-phase, all ice particles precipitate out of the cloud, turning the mixed-phase back into liquid. In other words, the thermodynamic phase evolution of such cloud can be described by the diagram: liquid => mixed-phase => liquid (i.e. (1)=>(2)=>(1)). The imbalance between the water vapor supply and the bulk ice mass crystal growth, required for the maintentenance of mixed-phase clouds, was discussed in Rauber and Tokay (1991), Pinto (1998). An interesting aspect of maintenance of supercooled liquid clouds was discussed by Westbrook and Illingworth (2011). There is a fair amount of modelling attempts to find an explanation of maintenance of mixed-phase clouds through the balance of INPs and dynamic forcing (e.g., Avramov, A., et al. 2011; Fan et al. 2009, 2011; Smith et al., 2009; to name a few). The second mixed-phase evolution scenario is related to the generation of mixed-phase clouds in a pre-existing ice cloud due to dynamic forcing, which can presented by a diagram ice=>mixed-phase (i.e. (4)=>(2)). Note, that Fig.2 considers stage (4) as a final stage, whereas in the second scenario, (4) is an initial stage. The theoretical basis explaining such process was developed in Korolev and Mazin, 2003; Korolev

and Field, 2008, Field et al. 2014; Hill et al, 2014). These studies were supported by earlier observations of mixed-phase clouds embedded in pre-existing, deep ice clouds (e.g., Hogan et al., 2002; Field et al. 2004). To summarize the above, the direction of the evolution of a mixed-phase environment may differ from the classical consideration (as in Fig.2), which was assumed in this work. Since the present study does not contain evidence justifying the classical evolution ((1)=>(2)=>(3)=>(4)) of the sampled mixed-phase clouds, it would be relevant to rewrite the sections of the paper discussing the "transition phases" and make a disclaimer of two other scenarios of the mixed-phase evolution.

We thank the reviewer for these very helpful and detailed comments on the possible transition/evolution pathways among liquid, mixed and ice phase clouds. We revised the conceptual diagram in **Figure 2** to illustrate these additional possible pathways, allowing the two-way transitions between each transition phase to occur.

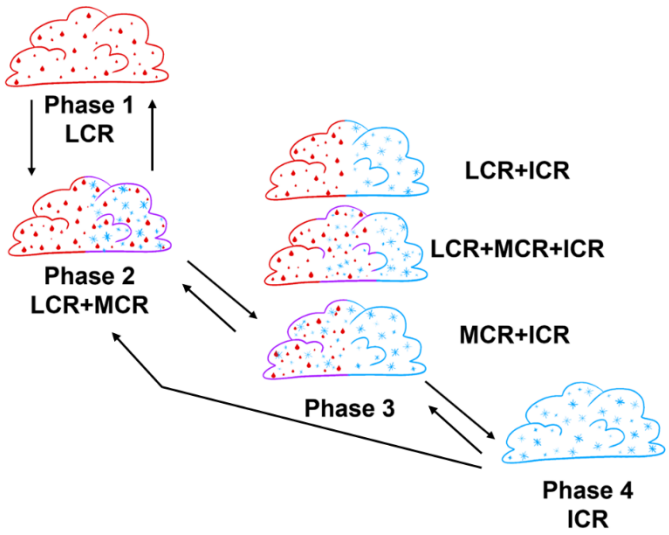

Figure 2. A conceptual diagram of the four transition phases for mixed-phase cloud evolution. Red, blue, and purple shading indicates liquid cloud region (LCR), ice cloud region (ICR) and mixed cloud region (MCR), respectively.

In addition, we added a paragraph in section 3.1 to discuss these pathways and provided more context of how the transition phases are related to the previous studies: "Several potential evolution pathways have been documented and discussed in previous literature, which can be linked with the separation of the four transition phases described above. A "classical" type of evolution pathway follows phases (1)=>(2)=>(3)=>(4), which was observed and documented over 35 years ago (e.g., Hobbs and Rangno, 1985). This type of evolution describes the situation that a cloud is initiated as liquid phase under supercooled conditions; then it experiences ice nucleation and turns into mixed-phase; after that some section of the mixed-phase cloud glaciates and turns into ice; and in the final stage, the entire cloud is glaciated. Besides the classical progression of mixed-phase, there are two other routes of evolution of mixed-phase clouds. The second pathway is when, after nucleation of INPs and turning liquid clouds into mixed-phase, all ice particles precipitate out of the clouds, turning the mixed-phase back into liquid. In other words, the thermodynamic phase evolution of such clouds can be described as liquid => mixed-phase => liquid, i.e., phases (1)=>(2)=>(1). The imbalance between the water vapor supply and the bulk ice mass crystal growth, required for the maintenance of mixed-phase clouds, was discussed in Rauber and Tokay (1991), Pinto (1998), and Westbrook and Illingworth (2011). There is a fair amount of modelling attempts to find an explanation of maintenance of mixed-phase clouds through the balance of

INPs and dynamic forcing (e.g., Avramov et al., 2011; Fan et al., 2009, 2011; Smith et al., 2009). The third pathway of mixed-phase evolution is related to the generation of mixed-phase clouds in a pre-existing ice cloud due to dynamic forcing, which can be presented as ice=>mixed-phase, i.e., phases (4)=>(2), or (4)=>(3)=>(2). Note that the numerical order of phases 1 – 4 does not necessarily represent the evolution direction. For example, phase 4 may either be the final stage in the first classical pathway, whereas in the third pathway, phase 4 is an initial stage. The theoretical basis explaining such process was developed in several previous studies (e.g., Korolev and Mazin, 2003; Korolev and Field, 2008, Field et al., 2014; Hill et al., 2014). These studies were supported by earlier observations of mixed-phase clouds embedded in pre-existing, deep ice clouds (e.g., Hogan et al., 2002; Field et al., 2004). We caution that a mixed-phase cloud may or may not follow these exact pathways in the real atmosphere, as certain transition phases may be skipped, the evolution direction could be reversed, and multiple phases can appear in the same cloud in a 3-D view. Nevertheless, this method provides a statistical separation of the cloud transition phases and allows a more focused analysis of the coexistence of supercooled liquid water and ice crystals that cannot be achieved solely based on second-by-second measurements (i.e., if one only analyzes seconds with coexisting ice and liquid)."

2. As follows from the explanation in section 3.1, this study considers two types of mixed phase clouds as "genuine" where ice particles and liquid droplets are spatially mixed on a small scale, and "conditionally" mixed clouds, where ice and liquid are spatially separated (see Korolev et al. 2017 (Fig.5-1); Korolev and Milbrandt, 2022 (Fig.1)). In conditionally mixed-phase clouds the WBF process is disabled due to spatial separation of ice and liquid. Thus, the clouds identified in this study as (3), may form a sequence of spatially adjacent cloud segments ...-ice-liquid-ice-liquid-... Such clouds are thermodynamically stable, and their lifetime will be determined by processes other than the interaction between ice and liquid (e.g., WBF, riming). Therefore, the term "transition phase" is not directly applicable to the "conditionally" mixed clouds considered in this paper, and it is relevant only to "genuinely" mixed-phase clouds. On the same note, in the frame of classical consideration of the mixed-phase evolution, the ice stage (4) is stable; (in terms mixed-phase transformation, other types of instabilities are not considered). Therefore, the term "transition phase" should not be applied to stage (4). Having said that, the term "transition phase" should be reconsidered in this study and used cautiously and applied only to "genuinely" mixed clouds.

We thank the reviewer for pointing out the stability of some conditions compared with others. We would like to point out that the scenario of "LCR+ICR" is one of the three scenarios for phase 3, since phase 3 can also have "LCR+MCR+ICR" and "MCR+ICR". The conditionally mixed phase clouds (i.e., represented by LCR+ICR) only contribute to 840 seconds out of the total 11988 seconds of phase 3.

We added more discussion about this in section 4: "The definition of LCR, MCR and ICR is also related to the two types of mixed-phase clouds – genuinely versus conditionally mixed, separated by the level of mixing between supercooled liquid water and ice crystals (e.g., Korolev et al., 2017, their Fig. 5-1; Korolev and Milbrandt, 2022, their Fig. 1). The scenario of "LCR+ICR" identified as one sub-category in phase 3 would be considered a conditionally mixed-phase cloud, which may form a sequence of spatially adjacent cloud segments ...-ice-liquid-ice-liquid-.... Such clouds may be thermodynamically stable, and their lifetime would be determined by processes other than the interaction between ice and liquid (e.g., WBF and riming). This special scenario when only "LCR+ICR" exist in the TCR without the existence of MCR has 840 seconds of samples, which is a small fraction of the total 11988 seconds of transition phase 3 samples. This result suggests that most of the clouds with coexisting supercooled liquid water and ice particles at least contain some partial segments as genuinely mixed phase, i.e., MCR."

3. Since the direction of the evolution of mixed-phase environment may go backward, in contrast to the classical evolution, it makes sense to consider the microphysical properties of cloud thermodynamic

states (1-4) without connection to the evolution of mixed-phase or to do so cautiously. This may also involve changing of the title of the paper.

We have rewritten the manuscript carefully, to tune down the description of the cloud evolution direction, but rather focus on these transition phases as various stages of clouds. Since we have revised the cartoon diagram of Figure 2 as illustrated above, the transition phases are not limited to a single direction of evolution but allow two-way transitions and a cycle between these phases. In addition, we changed the title of the manuscript to: "Transition between ~~from~~ Supercooled Liquid Water and ~~to~~ Ice Crystals in Mixed-phase Clouds based on Airborne In-situ Observations".

Because of this, we feel that the transition phase term does not indicate a specific connection with the evolution direction of the clouds anymore, and therefore we keep using the term.

Data quality

I have some concerns regarding the results of the particle size distributions (PSD), humidity and vertical wind measurements presented in this paper. The details are described below.

4. Measurements of DSD in liquid clouds (red lines):

(a) The DSDs, measured by the 2DC in liquid clouds in all temperature subranges (including -30<T<-20C and -40<T<-30C), extend up to 3mm in diameter. These are exceptionally large raindrops for stratiform clouds at temperatures below -20C. To my best knowledge, I have never seen reports of observation of 2-3mm supercooled raindrops at -40<T<-20C.

(b) As follows from Fig. 6, the concentration of supercooled drops with D>200um measured by 2DC in liquid clouds (red lines) appears to be higher than the concentration of ice particles measured in mixed-phase clouds (light green lines) by 2DS. At temperatures -40<T<-20C (Figs.6c,d) the concentration of drops D>~2mm measured by 2DC is higher than the concentration of ice particles in ice clouds. Such behaviour appears to be anomalous.

(c) Dmax measured by 2DS and 2DC are expected to be approximately close to each other. This statement is well satisfied for PSDs in cloud types (2), (3) and (4) in Figs. 5 & 6. However, in liquid clouds (type (1)) there is a well pronounced difference between Dmax measured by the 2DS (~300um) and that measured by the 2DC (~3mm).

Items (a)-(c) are indicative that the SLD measurements by 2DC in liquid clouds are compromised.

We thank the reviewer for giving us detailed comments on the data quality of various measurements. Regarding the large particles reported by 2DC in the original PSD figures, we conducted a comparison between Fast-2DC and 2DS probes for each research flight using time series and statistical comparison. We concluded that the Fast-2DC measurements had issues with particle imaging during various flight segments in SOCRATES and decided to exclude Fast-2DC probe from this analysis. Nevertheless, our main analysis relies on the other two probes (i.e., 2DS and CDP) and the main conclusion is not affected by the exclusion of Fast-2DC.

5. The 2DS DSD in Fig.6a,c,d in the temperature subranges -10<T<-0C, -30<T<-20C and -40<T<-30C appear to be nearly the same. All three DSDs have the same Dmax=~300um. Based on the past in-situ observations the concentration of SLD and Dmax is expected to decrease with the decrease of temperature due to an increasing of the probability of droplet freezing with the decrease of T and

increase of their D. Both the absence of the temperature dependence of 2DS DSDs and observations of SLDs with D~200-300um below -30C are highly questionable.

We thank the reviewer for pointing out these detailed features. We applied the following revisions to address the reviewer's question of erroneous, large liquid particles measured by 2DS with diameter > 200 micron in phase 1. Previously, we defined 2DS detected particles with D_{max} (maximum dimension in a second) greater than 312.5 micron as ice particles, following the same definition described in D'Alessandro et al. (2019) in their Figure 1. For particles with D_{max} between 112.5 and 312.5 micron, they are defined as liquid if the standard deviation of particles within that second (σ_D) ≤50 micron, and as ice if σ_D > 50 micron. That is, if a particle has diameter > 200 micron, it can be either ice or liquid as the reviewer pointed out. In the revised method, we restrict particles with D_{max} > 212.5 micron to be ice particles, reducing the large particles being categorized as liquid droplets. The revised PSD in the new **Figure 6** is copied below. The 2DS measurements in phase 1 show maximum dimensions up to 212.5 micron. Phase 4 does not show CDP measurements since ice particles detected by CDP are excluded from this analysis.

We added the explanations to section 2.2: "Two modifications are applied to the previous cloud phase identification method of D'Alessandro et al. (2019) and Yang et al. (2021). The first modification is that only when CDP measurements are categorized as liquid droplets, these samples are used in the analysis. Measurements categorized by CDP as ice particles are excluded since previous work has shown that these measurements related to counting ice are most likely artifacts (e.g., Korolev et al., 2013). The second modification is about the treatment of large particles identified as liquid droplets. The previous method restricts particles with maximum dimensions (D_{max}) > 312.5 μm as ice particles, while those with D_{max} between 112.5 and 312.5 μm can be either liquid or ice depending on the standard deviation of particle sizes measured by 2DS in that second. In this work, we further restrict particles with D_{max} > 212.5 μm to be ice particles, reducing the number of large particles being categorized as liquid droplets."

Regarding the comment about temperature dependence of PSD, upon a closer examination, we found that phase 4 (blue line in Figure 6) shows decreasing frequencies of large ice particles with decreasing temperatures. For example, particles with 3000 μm dimension shows that dN/dlogDp value in the y axis decreases from 10^{-4} to 10^{-6} when temperature decreases (new Figure 6 a – d). But for phase 3, where ice particles still coexist with liquid droplets, it shows almost no trend of decreasing D_{max} with decreasing temperature. Our speculation is that since phase 3 still has supercooled liquid water coexisting with ice, these ice particles may still be subject to growth via WBF process, vapor depositional growth if there is ice supersaturation, and/or riming. Thus, the ice particle growth process is less limited in phase 3 compared with phase 4. We added some discussions on this in section 3.3: "Phase 4 shows a trend of decreasing frequency of large ice particles (e.g., D_{max} > 2000 μm) with decreasing temperature, which could be due to an increasing probability of droplet freezing with decreasing temperature given the same dimension that reduces the available amount of large supercooled liquid droplets for glaciation or riming at lower temperatures. On the other hand, phase 3, which still has supercooled liquid water coexisting with ice particles, does not show such trend, probably because ice crystal growth may occur via various processes in phase 3, such as WBF process, glaciation, vapor depositional growth under ice supersaturation, and/or riming."

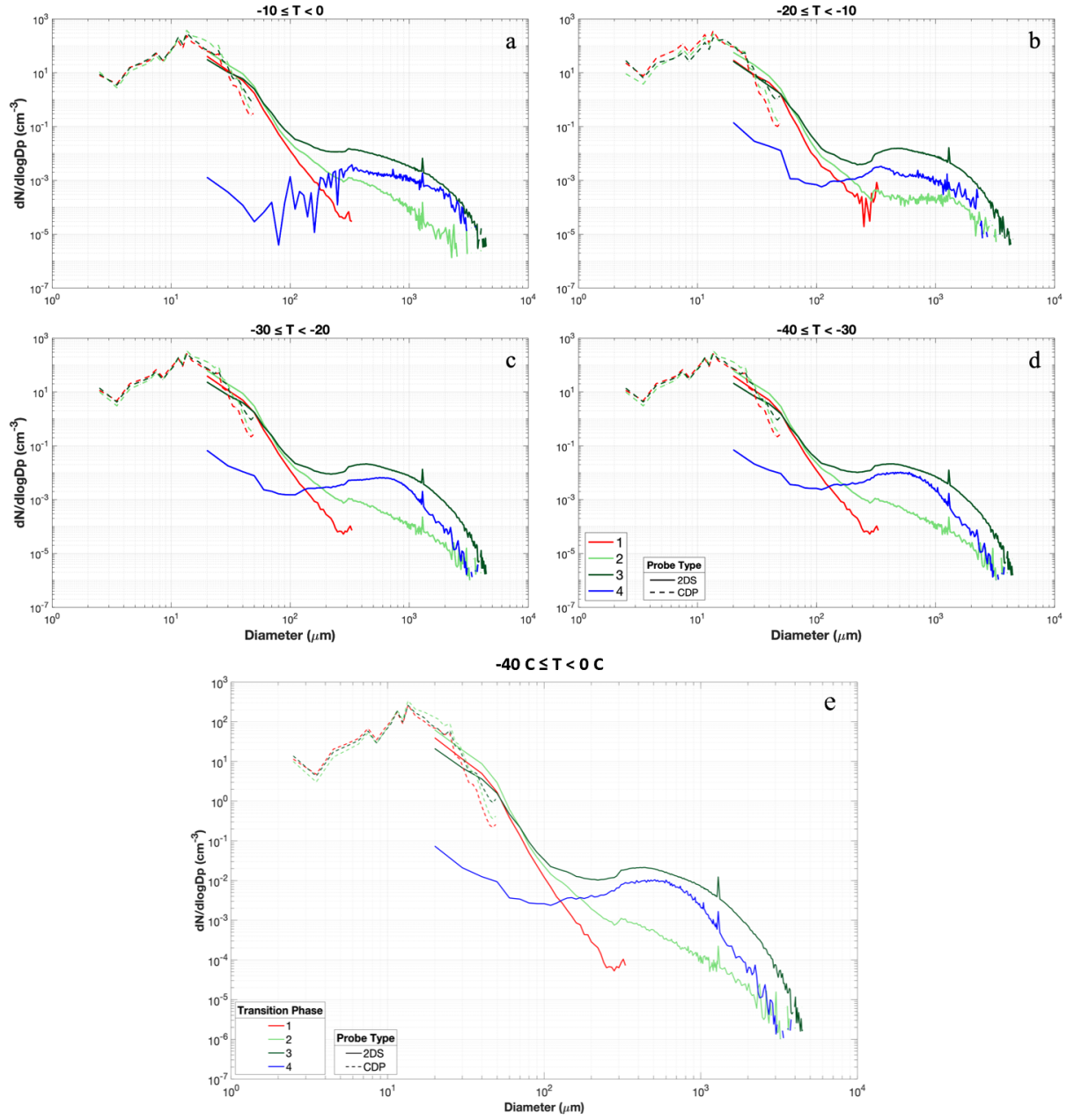

Figure 6. Particle size distribution of the four transition phases for mixed-phase clouds separated by probe types and temperature ranges. Phase 4 only shows 2DS measurements because ice particles measured by CDP are excluded from the analysis.

6. The particles counted by CDP in ice cloud (type (4)) are most likely artifacts related to counting ice (e.g. Korolev et al. 2013), and therefore, their contribution to ice should be excluded.

We agree with the reviewer and in the revised manuscript, all CDP measurements initially categorized as ice particles are excluded from the analysis. In other words, only CDP measurements categorized as liquid droplets are used. Section 2.2 is revised: "Two modifications are applied to the previous cloud phase identification method of D'Alessandro et al. (2019) and Yang et al. (2021). The first modification is

that only when CDP measurements are categorized as liquid droplets, these samples are used in the analysis. Measurements categorized by CDP as ice particles are excluded since previous work has shown that these measurements related to counting ice are most likely artifacts (e.g., Korolev et al., 2013)."

7. The diagrams in Fig.7 show observations of LWC in liquid clouds as low as 10-6 g/m3 (b), and IWC in ice clouds as low as 10-5.5 g/m3 (h). Such low LWC and IWC values are below the minimum threshold, which can be measured from aircraft at 1s-averaging time by the particle probes employed in this study (e.g. Baumgardner et al. 2017).

Following the suggestion of the reviewer, we revised the thresholds of in-cloud conditions to a higher threshold of total water content (TWC), described in section 2.1: "In-cloud conditions are defined as the 1-Hz measurements with total water content (TWC = IWC+LWC) greater than 0.001 g m^{-3}. Lower IWC and LWC values have also been reported by the two probes, but the threshold of 0.001 g m^{-3} is chosen here due to the larger uncertainties of these cloud probes reporting lower mass concentrations of hydrometeors (e.g., Baumgardner et al., 2017)."

In addition, we compared the impacts of using different IWC and LWC values as in-cloud thresholds in **supplemental Figures S2 and S3** (copied below). The analysis shows that using IWC or LWC thresholds of 10^{-6}, 10^{-5}, 10^{-4}, and 10^{-3} g m^{-3} do not show significant differences in the number of samples of four phases.

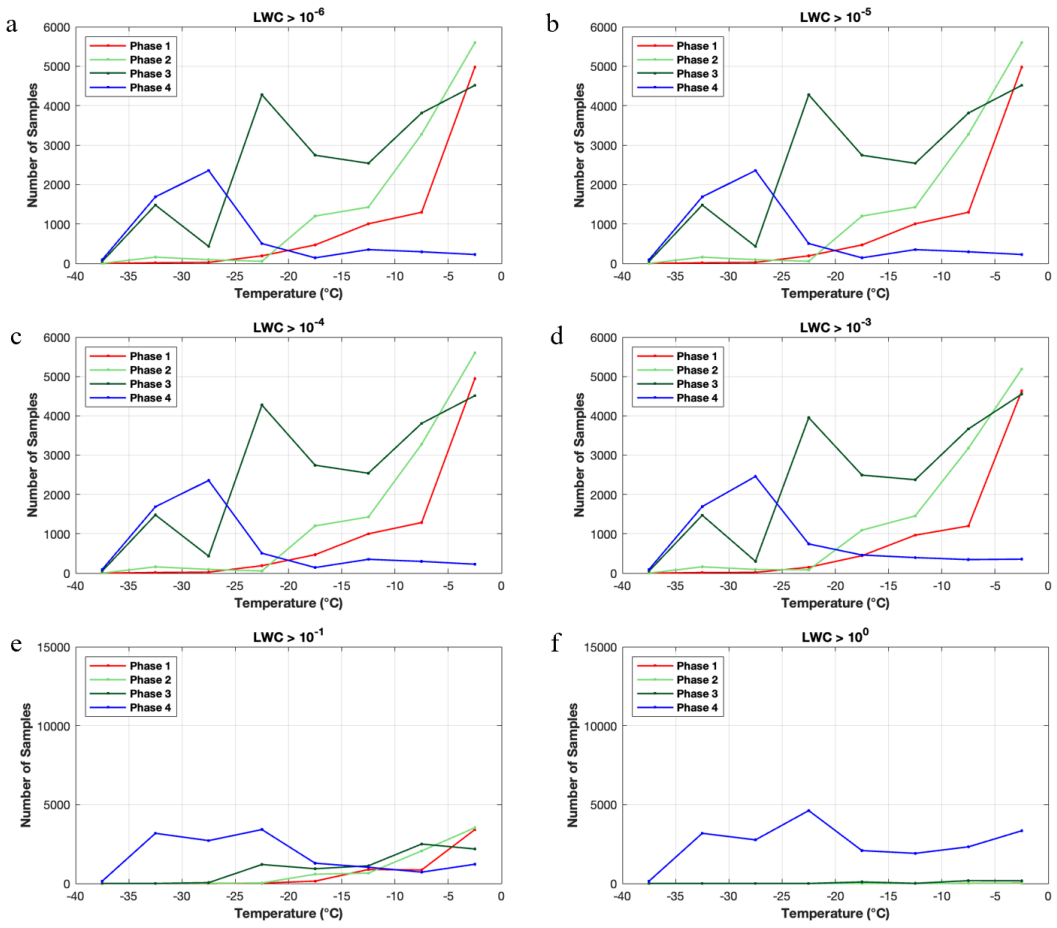

Figure S2. Similar to Figure 3 a, number of samples for four transition phases but using different liquid water content (LWC) values (unit: g m^{-3}) as the threshold for defining in-cloud conditions.

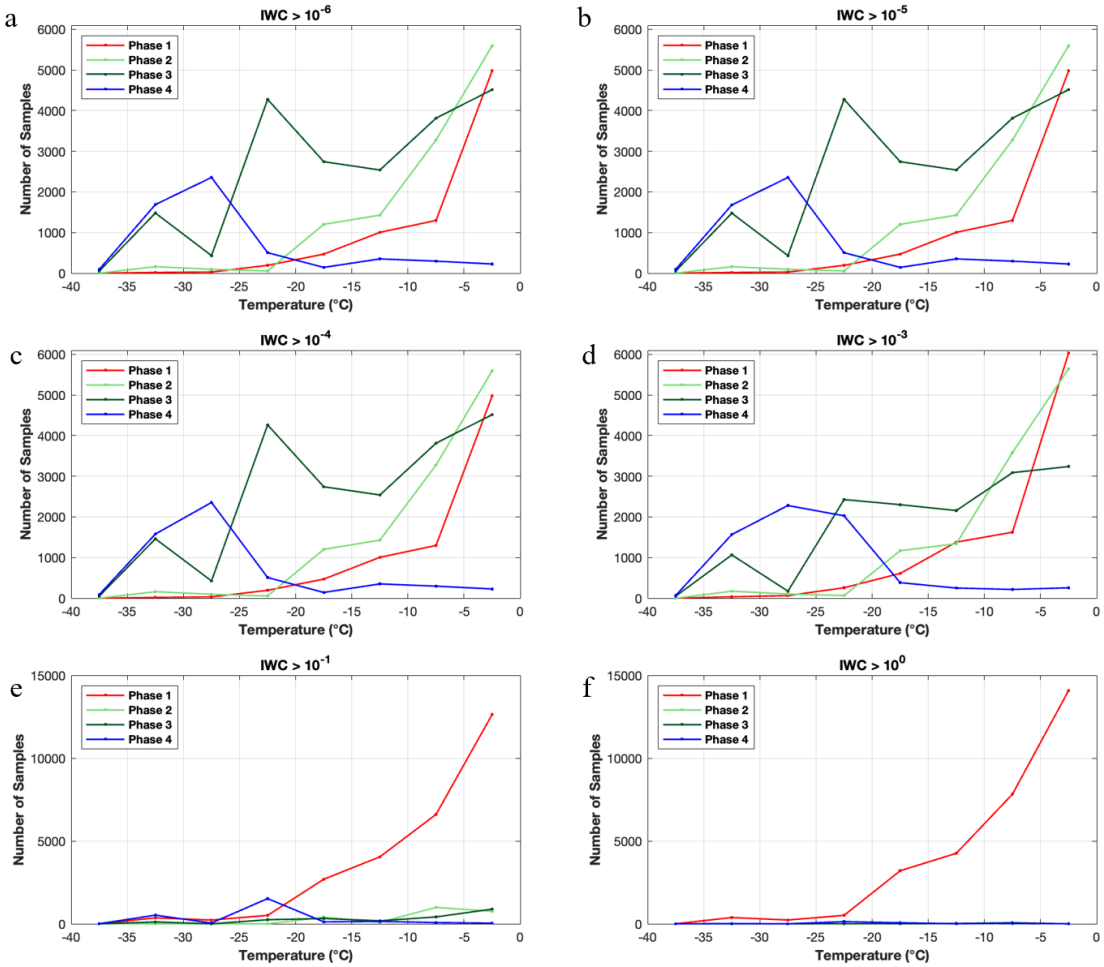

Figure S3. Similar to Figure 3 a, number of samples for four transition phases but using different ice water content (IWC) values (unit: g m^{-3}) as the threshold for defining in-cloud conditions.

8. Both theoretical and observational studies (Korolev and Mazin, 2003; Korolev and Isaac, 2006) showed RHliq in mixed phase clouds is close to 100%. Due to the short time of phase relaxation (typically 0.1-10s) in liquid and mixed-phase clouds, the evaporating droplets will rapidly bring the system of "droplets-water vapor" to quasi-equilibrium and saturate the environment. In this regard, the observations at -25C in liquid and mixed-phase clouds (with no ice) of RHliq ~88%, 82% and 75%, respectively (Fig.10b), is suggestive of large biases in RHliq measurements. The low accuracy of RHliq does not allow for the conclusions made in the paper about the relationships between humidity and microphysical parameters of cloud type (1)-(4).

We appreciate the concern from the reviewer. We took a few approaches to address the concerns about the relative humidity measurements.

First, we would like to mention that in the summer of 2016 and 2018, we spent 3 months each year at the National Center for Atmospheric Research / Earth Observing Laboratory (NCAR/EOL) to conduct laboratory calibration of the VCSEL water vapor hygrometer. Below is a schematic diagram (**Figure R2-1**) and some results based on these calibrations. Even though such laboratory calibration has improved the original water vapor data, we note that combining the uncertainties from temperature data and water vapor data, the RHi and RHliq data would still have about 6% - 7% uncertainties.

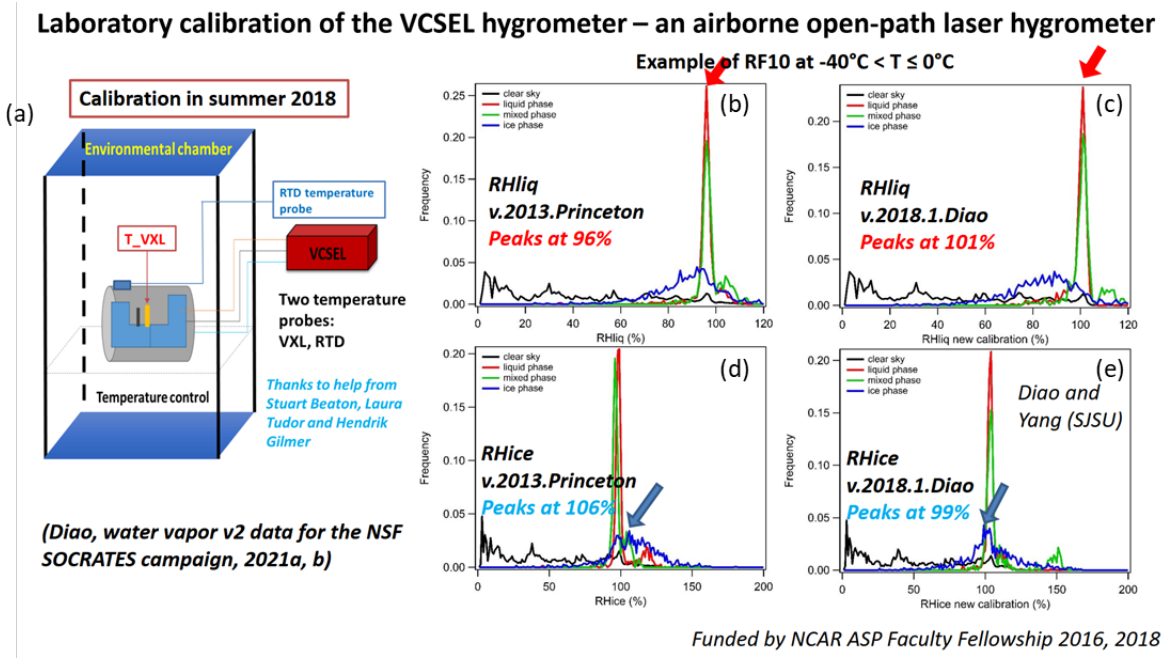

Figure R2-1. Laboratory calibration of the VCSEL hygrometer conducted by M. Diao. (a) A schematic diagram of the calibration system using the NCAR EOL environmental chamber. (b-e) An example of RH frequency distribution for research flight 10 in the NSF SOCRATES campaign. (b) RHliq frequency distribution that peaks at 96% for liquid and mixed phase clouds and (d) RHice frequency distribution that peaks at 106% for ice phase clouds using the older calibrations from Minghui Diao and Josh DiGangi at Princeton University in 2013. (c) New RHliq and (e) RHice frequency distributions using the Diao (2021) calibration for the SOCRATES campaign that peak at 101% and 99%, respectively. The new calibration of Diao (2021) has improved the peak position of RHliq and RHice for in-cloud conditions.

Second, we have noticed that the sub-saturated conditions for in-cloud conditions are detected not only by several NSF flight campaigns using the VCSEL hygrometer, but also by several other campaigns using completely different instruments and aircraft platforms. We speculate that there is some real physical explanation for these sub-saturated conditions. For example, it is possible that within a 1-second aircraft measurement, which is usually ~200 m resolution, the liquid droplets inside this segment may not immediately equilibrate with the entire volume of this segment for it to reach liquid saturation. In **Figure R2-2** below, we show the probability density function (PDFs) of RHi for three flight campaigns, NSF SOCRATES, NASA SEAC4RS and DOE ACME-V campaigns. We noticed that using two thresholds to define in-cloud conditions, i.e., TWC > 10^{-5} or > 10^{-3} g m^{-3}, the in-cloud RHi frequency distributions consistently show some subsaturated conditions. The NASA SEAC4RS campaign was based on NASA DC-8 research aircraft, and the water vapor was measured by the NASA Diode Laser Hygrometer (DLH) instrument. The DOE ACME-V was based on the DOE Gulfstream-1 research aircraft, using the Cavity Ring Down (CRD) instrument to measure gas phase including water vapor. This research topic regarding the high-resolution spatial variability of water vapor in relation to the spatial heterogeneity of the cloud hydrometeor distribution would be an interesting topic for high-resolution observations or LES simulations. However, limited by the available 1-Hz measurements in the SOCRATES campaign, we feel that testing such hypothesis on the existence of subsaturated conditions at sub-1 Hz resolution requires another study using different types of datasets at higher resolution. Nevertheless, we quantified the impacts of these sub-saturated conditions on our main conclusions in this work, which is discussed in the following paragraph.

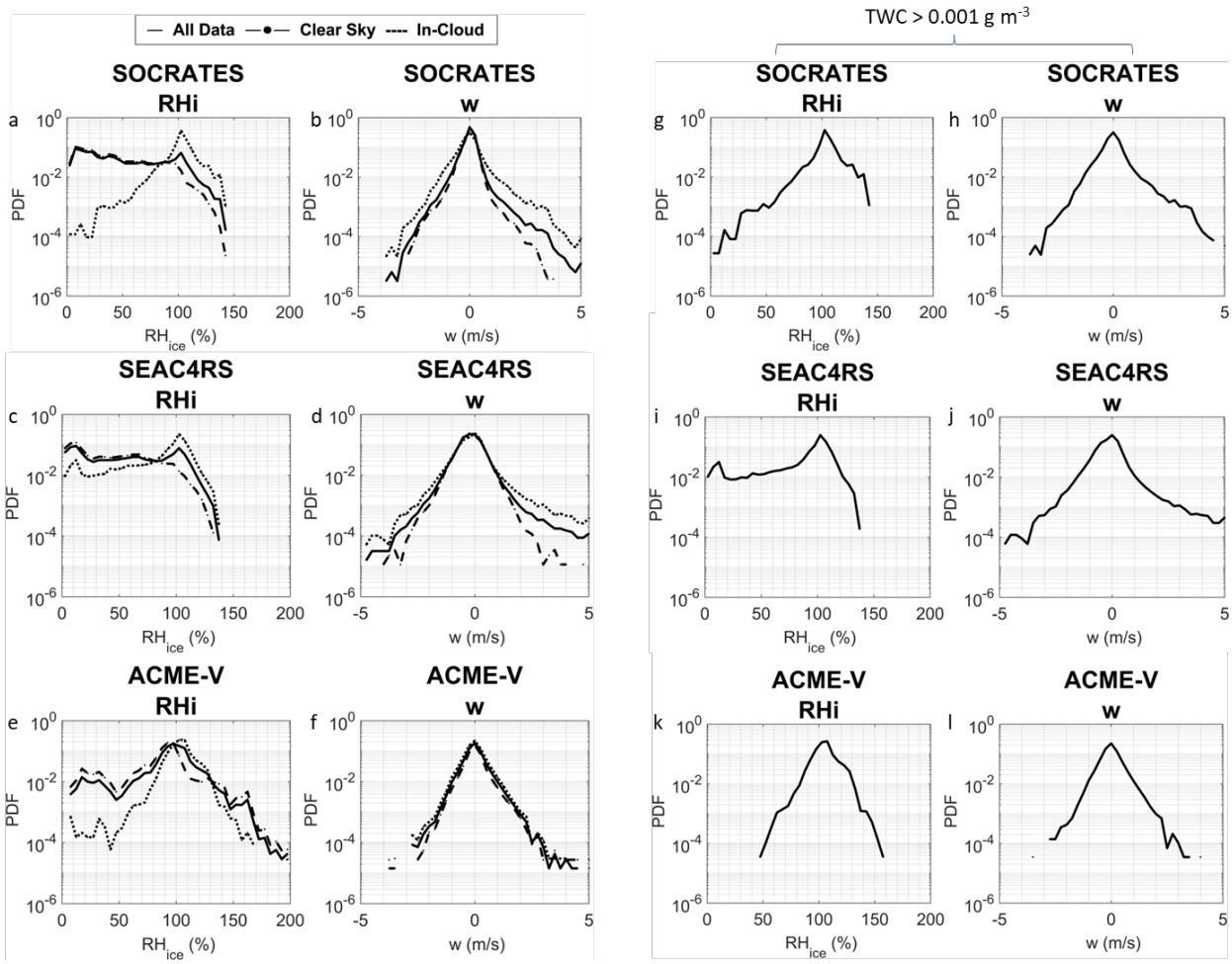

Figure R2-2. Probability density functions (PDFs) of RHi and vertical velocity for three flight campaigns – NSF SOCRATES, NASA SEAC4RS and DOE ACME-V. (a-f) Clear-sky, in-cloud and all-sky conditions, with in-cloud conditions defined by TWC > 10^{-5} g m^{-3}. (g-l) Similar to the left panels but using TWC > 0.001 g m^{-3} as the in-cloud threshold.

Third, we conducted a sensitivity test to the number of samples of four phases in **supplemental Figure S4**, using different restrictions of RH_i data, i.e., RH_i greater than 50%, 70%, 75%, 80%, 85%, and 90%. The results show similar distributions for the number of samples among these restrictions especially for RH_i > 70%. In addition, for the main analysis, we applied a sensitivity test using only RH_i > 80% and the results are shown in **supplemental Figures S7 – S9**, which are very similar to the results shown in Figures 7, 8 and 9, respectively. We contrast these analyses below in **Figure R1-1, R1-2, and R1-3**.

In summary, even though we cannot 100% verify the reasons behind these sub-saturated conditions for in-cloud samples, either including or excluding these sub-saturated conditions does not show a large impact on our main conclusions, which indicates that these main results are robust. We added a comment on these sub-saturated conditions in section 3.2: "For phase 1, a small amount of ice sub-saturated conditions is seen. Besides the 6% – 7% uncertainties in RH_i values that originate from the combination of water vapor and temperature measurement uncertainties, the deviation of relative humidity from liquid saturation line may be due to spatial variability of RHi at sub-1 Hz resolution and/or lower LWC to provide sufficient vapor-liquid phase equilibrium at a 200-m scale."

We also added comments in section 3.2: "Previous theoretical and observational studies (Korolev and Mazin, 2003; Korolev and Isaac, 2006) showed that RH_{liq} in mixed-phase clouds is close to 100%, due to evaporating droplets rapidly via the WBF process, bringing the system of "droplets-water vapor" to quasi-equilibrium and therefore saturating the environment. As liquid droplets glaciate into ice particles, the peak of RH frequency would also shift towards ice saturation (e.g., D'Alessandro et al., 2019). The in-cloud samples used in this study contain some sub-saturated conditions that deviate from liquid saturation in phases 1 – 3 or from ice saturation in phase 4 (as shown in Figure 4 a – d), which may be attributed to a combination of reasons, such as 6%–7% uncertainties in RH values originated from water vapor and temperature measurement uncertainties, heterogeneous distributions of LCR, MCR and ICR that lead to an uneven distribution of supercooled liquid water, as well as non-equilibrated states between vapor/liquid or vapor/ice phase due to a larger volume being sampled by fast aircraft measurements (~172 m horizontal resolution for 1-Hz measurements used here)."

Also in section 3.3: "To assess the impacts of the sub-saturated conditions within TCR on the main findings of this work, we examine the impacts of excluding the lower RH_i samples from the analysis of cloud micro- and macrophysical properties. Supplemental Figures S7 and S8 show the results of excluding $RH_i < 80\%$ based on the analysis similar to Figures 7 and 8, respectively. The relationships of ice particle number fraction, IWC, LWC and ice mass fractions with respect to mixed spatial ratio and ice spatial ratio show similar results when lower RH_i are excluded, demonstrating the robustness of these main conclusions."

We also commented in section 3.4: "The analysis of Figure 9 is also conducted for only $RH_i > 80\%$ in supplementary Figure S9 and the results show consistent results of the cloud phase frequency distributions regardless of the exclusion of low RH_i values."

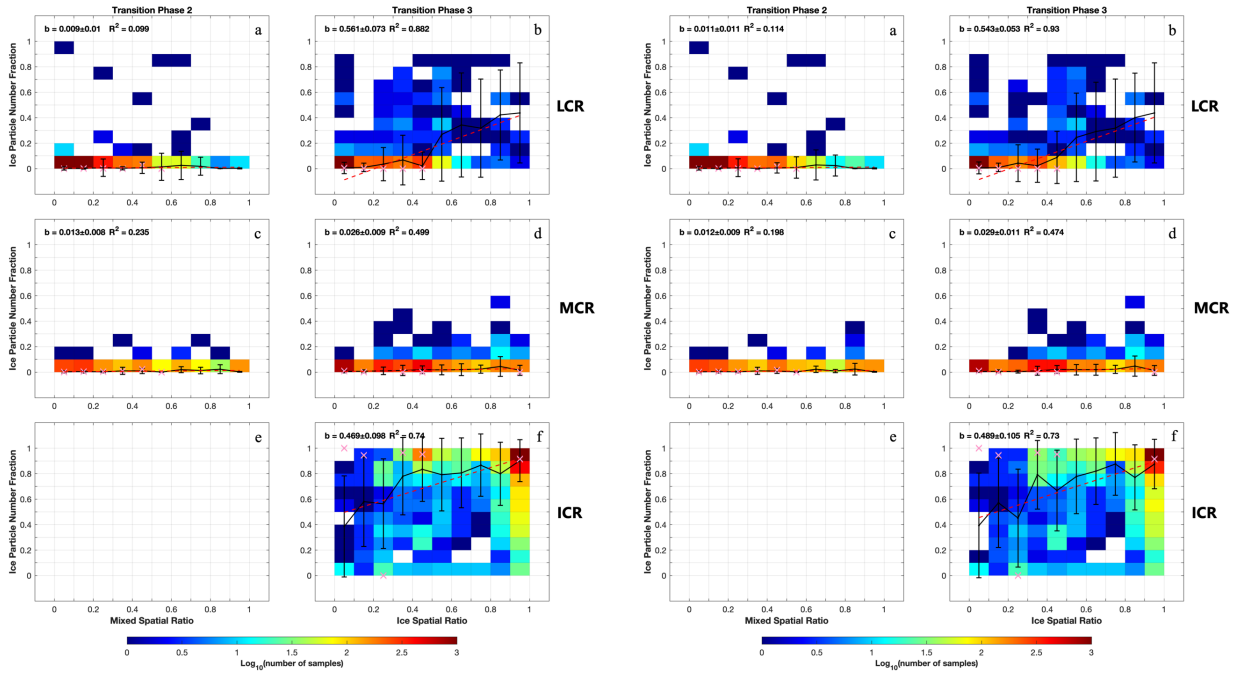

Figure R1-1. Side-by-side comparisons of using all RH_i data (left) versus using only high RH_i (>80%) (right). The figure on the left is Figure 7, on the right is Figure S7.

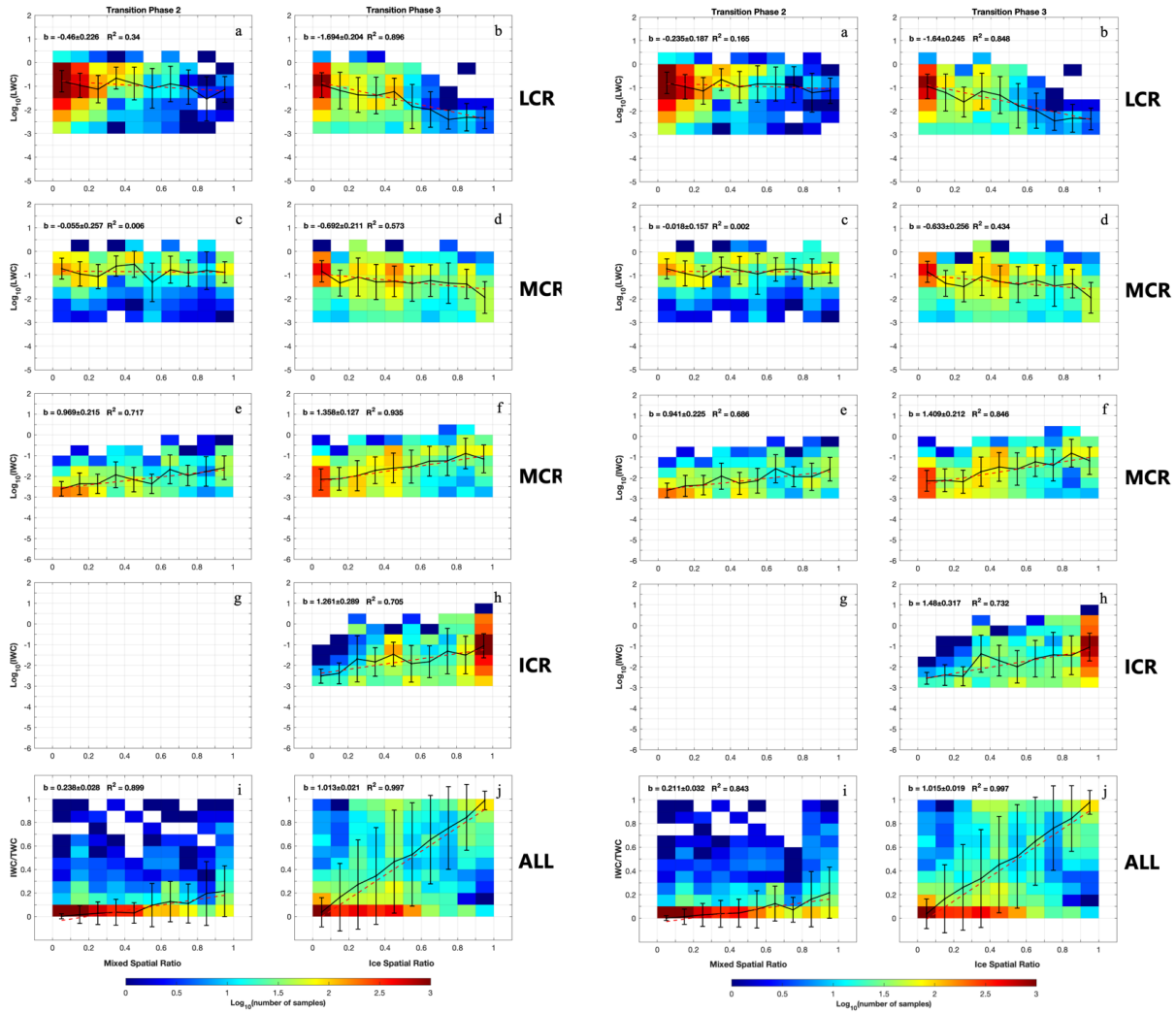

Figure R1-2. Side-by-side comparisons of using all RH_i data (left) versus using only high RH_i (>80%) (right). The figure on the left is Figure 8, on the right is Figure S8.

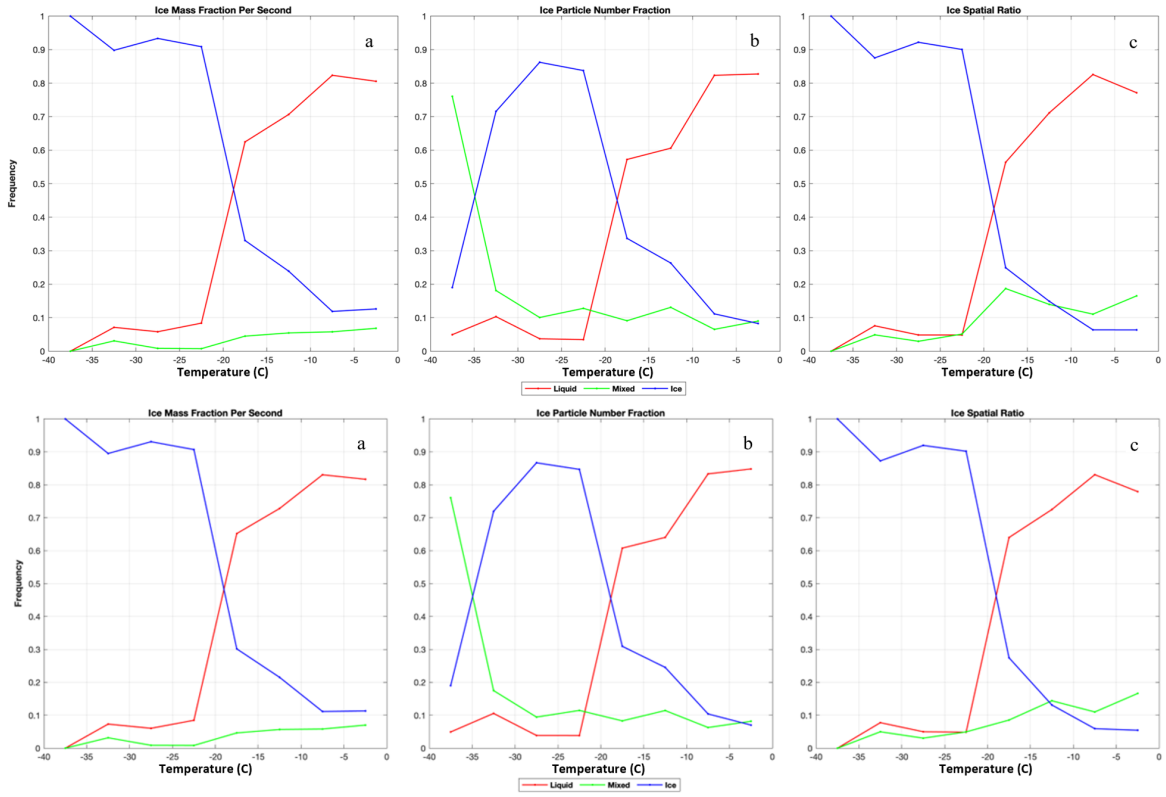

Figure R1-3. Side-by-side comparisons of using all RH_i data (top) versus using only high RH_i (>80%) (bottom). The figure on the top is Figure 9, on the bottom is Figure S9.

9. Numerous in-situ observations (including those, cited in the present study e.g., Wang et al. 2020) showed that in stratiform clouds the distribution of the vertical wind is centered close to zero. A visual assessment of the diagram in Fig.10c suggests systematic biases of the vertical wind with an average speed of ~-0.2m/s or lower. For mixed-phase clouds (type 2) at -25C the biases in vertical wind reached -0.5m/s and ~-0.9m/s. Clouds subsiding at such speed are expected to evaporate within a relatively short time due to adiabatic heating. Thus, for LWC(0)=0.1g/m3 at -10C, a cloud parcel descending at 0.2m/s will evaporate within 8 minutes.

We thank the reviewer for this inspection of the vertical velocity. We examined the distributions of vertical velocity for clear-sky, in-cloud, and all-sky conditions more closely and decided to apply a adjustment of +0.125 m/s to the 1-Hz vertical velocity observations. After this correction, the PDFs of velocity in are now centered at 0 m/s, which are illustrated **Figure R2-2** above as well as in supplemental **Figure S6**. This correction is mentioned in the main text in section 2.1: "The vertical velocity measurements are derived from several instruments, including Honeywell LASEREF IV Inertial Reference Unit, radome pressure, static pressure, pitot tubes, temperature probe, and differential Global Positioning System with an accuracy of ~±0.15–0.30 m/s and precision ~0.01 m/s (Diao et al., 2015). When examining the in-cloud and clear-sky conditions in the SOCRATES campaign, we noticed a low bias of the original vertical velocity measurements, and therefore applied a correction of +0.125 m/s for the vertical velocity values. After this correction, the peak of the frequency distributions of vertical velocity is centered at 0 m/s for both in-cloud and clear-sky conditions." After correcting the w distributions, the original Figures 9 and 10 are now updated and combined into the new **Figure 5** (below).

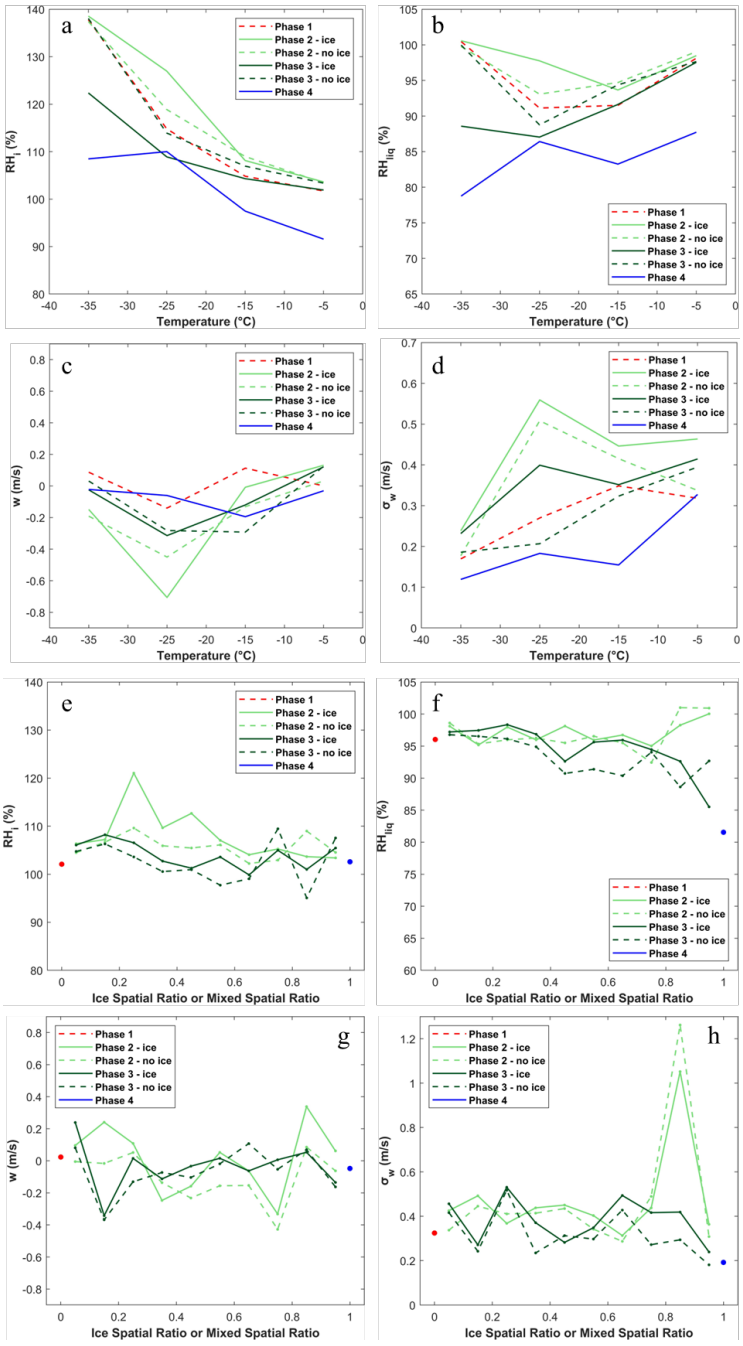

Figure 5. Distributions of (a) RH_i, (b) RH_{liq}, (c) vertical velocity (w), and (d) standard deviation of vertical velocity (σ_w) for various transition phases at different temperatures. (e-h) Similar to (a-d), but in relation to various mixed spatial ratios or ice spatial ratios. Phases 1 and 4 show ice spatial ratio at 0 and 1, respectively, and therefore only a single dot is shown for phases 1 and 4 in (e-h).

In addition, we would like to note that even though the mean w values seem to have more downdrafts when plotting w against ice spatial ratio or mixed spatial ratio (new Figure 5), the number of samples are not evenly distributed in various bins of ice spatial ratio or mixed spatial ratio (new **supplementary Figure S5**). In fact, the PDF of w shows higher frequencies of updrafts than downdrafts for phases 1 – 3 (**Figure S6 b**). We added discussion on this point in section 3.2: "The mean values of w do not vary

significantly with mixed spatial ratio or ice spatial ratio (Figure 5 g), but the PDFs of vertical velocity in supplemental Figure S6 b show higher frequencies of updrafts for phases 2 and 3 compared with phases 1 and 4, meaning that the segments containing both supercooled liquid droplets and ice particles are subject to relatively more updrafts, compared with the segments containing only liquid droplets or only ice crystals. This finding is consistent with Shupe et al. (2008) which pointed out the importance of updrafts for sustaining mixed-phase clouds. Differing from the previous studies, our method can further specify that the highest updrafts and vertical velocity fluctuations are found in transition phase 3 when pure ice segments start to appear (~4.5 m/s in Figure S6 b and ~2.3 m/s in Figure S6 c), consistent with the fact that RH_{liq} deviates more from liquid saturation in phase 3 (Figure 5 f), and therefore higher updrafts would be required to maintain supercooled liquid droplets."

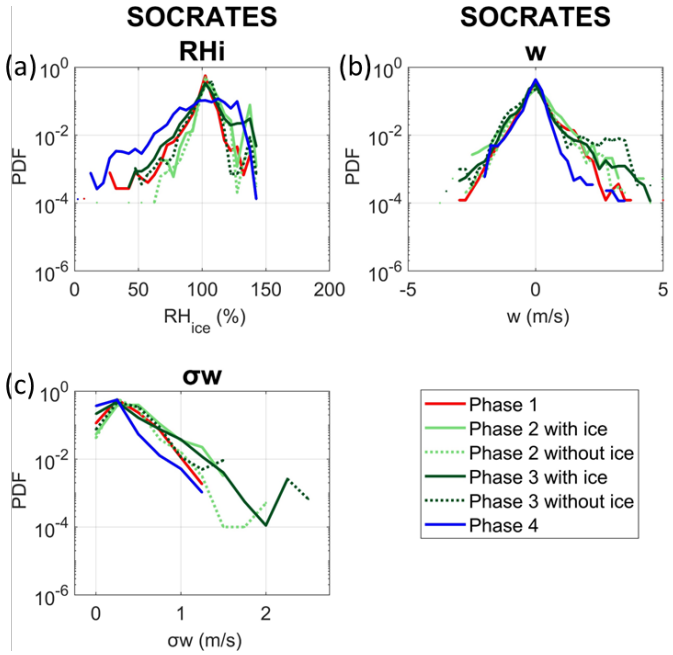

Figure S6. Probability density functions (PDFs) of (a) relative humidity with respect to ice, (b) vertical velocity (w), and standard deviations of w (σ_w) separated by different transition phases. Phases 2 and 3 are further separated into seconds with or without ice in this analysis. Both phases 2 and 3 show higher frequencies of updrafts and σ_w compared with phases 1 and 4.

Clarity or presentation

There are several items that require an explanation or need a more detailed description.

10. What is the definition of a cloud employed in this study? E.g., LWC>X, or N>Y or something else?

We define a 1-Hz sample as in-cloud condition when the TWC is greater than 0.001 g m^{-3}.

11. In section 3.1, I had a hard time understanding what the total cloud region (TCR) is. Is it a cloud separated from other clouds by a clear sky segment? Or is it an entire cloud domain sampled during a field campaign? If it is the latter, was a cloud free environment included in the statistics? If TCR refers to separate clouds, then how was the calculation of cloud statistics performed? i.e., were TCRs normalized on their spatial extension?

TCRs are individual, separate segments that are surrounded by clear-sky conditions. Each second within a TCR is counted as one 1-Hz sample, and all seconds are used in the rest of the analysis (e.g., new Figures 3 – 10) in this manuscript. We agree that this is an important concept and should be explained more clearly. We added a **supplemental Figure S1** and explained this in section 3.1: "In the second step, a total cloud region (TCR) that can potentially contain a combination of LCR, ICR and MCR is identified, which basically is a consecutive in-cloud segment surrounded by clear-sky conditions. If a TCR sample is surrounded by two adjacent seconds of NaN, then this sample is deleted, because one cannot determine if the NaN points are the edge of the cloud or if they are still part of the cloud. But if a TCR sample is surrounded by two adjacent seconds of clear-sky samples, then this in-cloud sample is valid, and its measurement can last from one second to many seconds. For instance, if five seconds of LCR are adjacent to one second of MCR, then both the LCR and MCR belong to the same TCR. An illustration of the identification of TCR is shown in supplemental Figure S1. All the 1-Hz samples within the TCR are used in the analysis in the following sections."

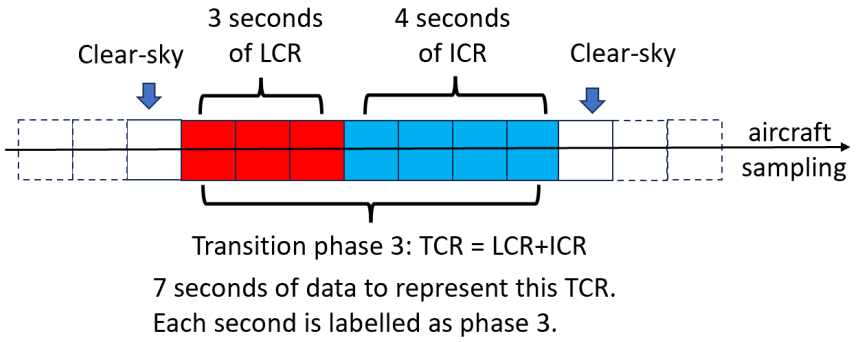

Figure S1. A schematic diagram that illustrates the identification of a total cloud region (TCR) sample, with liquid cloud region (LCR) and ice cloud region (ICR) embedded inside this TCR. All 7 seconds of samples inside this TCR are used in the analysis of cloud properties.

12. Definition of mixed-phase clouds:

(a) The definition of mixed-phase based on LWC (or IWC) mass fraction LWC/TWC (or IWC/TWC) has been used in the cloud physics community for approximately thirty years. It is worth acknowledging this in the paper.

We added acknowledgment on the history of this method in section 3.4: "This method of using ice mass fraction to define mixed-phase clouds has been used in the cloud physics community for approximately thirty years (e.g., Korolev et al., 1998; Korolev et al., 2017, their equation 5-1 and references therein)."

(b) The second definition of mixed-phase, based on particle concentrations, is Nliq/(Nliq+Nice), where Nliq and and Nice are the concentrations of droplets and ice particles, respectively. Since, for most clouds, Nliq is typically larger than Nice by 3 to 5 orders of magnitude, with a very few exceptions the ratio Nliq/(Nliq +Nice) ≅ 1. Therefore, since Nliq/(Nliq +Nice)>0.9, the majority of clouds should fall in the category of liquid clouds. This is clearly inconsistent with the results shown in the diagram on Fig.4b. This contradiction requires an explanation.

We thank the reviewer for catching this error. We initially made a mistake of not adding the CDP measured liquid droplets into the 2DS measured liquid droplets for calculating total liquid number

concentrations. We have corrected this mistake. The new **Figure 9** below shows higher liquid phase frequency when temperature is closer to 0°C using the ice number particle fraction method, compared with the other methods using ice spatial ratio or ice mass fraction.

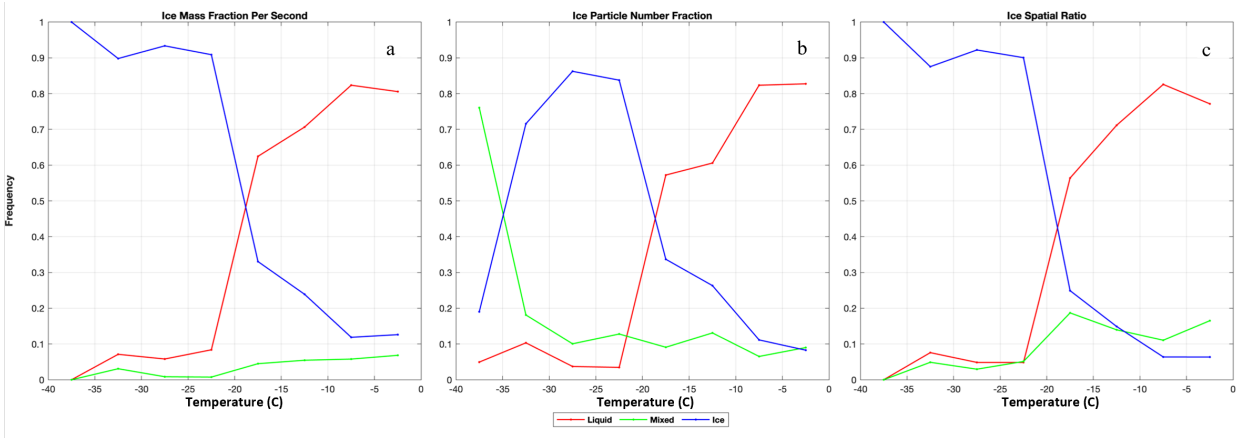

Figure 9. Cloud phase occurrence frequencies at various temperatures. Cloud phase identification methods are based on (a) ice mass fraction per second, (b) ice particle number fraction per second, and (c) ice spatial ratio calculated for individual consecutive TCR.

(c) The spatial ratio is defined as Length(cloud type)/Length(total). In this regard, the statement on line 165: " ...for each TCR, ice spatial ratio is calculated as length of (ICR+MCR) / length of TCR" sounds contradictory to this definition. If the definition of the spatial fraction is different from that stated above, then a more detailed explanation is required. Also, note that the spatial ratio was used for characterization of mixed-phase clouds in Korolev et al. (2017, Fig.5-13a).

We can see how our definition of spatial ratio may be confused with the other way of defining spatial ratios in the previous studies. We clarified in the last paragraph of section 3.1 that the spatial ratio is calculated for each TCR segment, not for the bulk measurement of many cloud segments in a temperature bin: "In addition, we define two terms – mixed spatial ratio and ice spatial ratio, to represent the spatial fraction of ice-containing clouds in phases 2 and 3, respectively. Specifically, the mixed spatial ratio represents the fraction of MCR as part of an individual, consecutive TCR in phase 2, calculated as length of MCR / length of TCR. Ice spatial ratio represents the fraction of ice-containing segments as part of an individual, consecutive TCR in phase 3, calculated as (length of ICR + length of MCR * IWC/TWC) / length of TCR. The contribution of MCR to ice spatial ratio in phase 3 is weighted by the ice mass fraction, giving the MCR a smaller weighting function compared with ICR since MCR contains higher fractions of supercooled liquid droplets. Note that the definitions of mixed spatial ratio and ice spatial ratio differ from the spatial ratio previously used for characterization of mixed-phase clouds in Korolev et al. (2017, Fig.5-13a). In that previous method, the spatial ratio of a certain phase (liquid, mixed or ice) is calculated as the number of samples of that phase divided by the total cloud samples in a certain temperature bin. In this work, the mixed spatial ratio and ice spatial ratio are calculated for individual TCR segments, and therefore each TCR would produce one value for mixed spatial ratio and one value of ice spatial ratio. These values of mixed spatial ratio or ice spatial ratio are applied to every 1-second sample within this TCR."

13. It would be beneficial for this work to discuss the effect of the WBF process and glaciation on the thermodynamic state of mixed-phase clouds. I found no mention of the glaciation process. The WBF was mentioned only once at the end of the paper.

We added the new Figure 4 about the thermodynamic conditions (i.e., RH_i distributions) for each transition phase, and added more comments on WBF and glaciation as mentioned above: "Previous theoretical and observational studies (Korolev and Mazin, 2003; Korolev and Isaac, 2006) showed that RH_{liq} in mixed-phase clouds is close to 100%, due to evaporating droplets rapidly via the Wegner-Bergeron-Findeisen (WBF) process, bringing the system of "droplets-water vapor" to quasi-equilibrium and therefore saturating the environment. As liquid droplets glaciate into ice particles, the peak of RH frequency would also shift towards ice saturation (e.g., D'Alessandro et al., 2019). The in-cloud samples used in this study contain some sub-saturated conditions that deviate from liquid saturation in phases 1 – 3 or from ice saturation in phase 4 (as shown in Figure 4 a – d), which may be attributed to a combination of reasons, such as 6%–7% uncertainties in RH values originated from water vapor and temperature measurement uncertainties, heterogeneous distributions of LCR, MCR and ICR that lead to an uneven distribution of supercooled liquid water, as well as non-equilibrated states between vapor/liquid or vapor/ice phase due to a larger volume being sampled by fast aircraft measurements (~172 m horizontal resolution for 1-Hz measurements used here)." We mentioned glaciation in several other places, such as in section 3.3: "The decreasing ice crystal concentrations per size bin from phase 3 to phase 4 may be caused by stronger aggregation, sublimation, and/or sedimentation of ice crystals in phase 4, as well as by stronger glaciation and/or secondary ice production in phase 3… Phase 4 shows a trend of decreasing frequency of large ice particles (e.g., D_{max} > 2000 μm) with decreasing temperature. This could be due to an increasing probability of droplet freezing with decreasing temperature given the same dimension that reduces the available amount of large supercooled liquid droplets for glaciation or riming at lower temperatures. On the other hand, phase 3, which still has supercooled liquid water coexisting with ice particles, does not show such trend, probably because ice crystal growth may occur via various processes in phase 3, such as WBF process, glaciation, vapor depositional growth under ice supersaturation, and/or riming."

14. The rapid increase of occurrence of ice clouds in the temperature range -15C to -20C was observed by other research groups (e.g., Wallace and Hobbs 1975; Moss and Johnson 1994; and others), which is worth acknowledging here.

We added this comment in the last paragraph of section 3.4: "The rapid increase of occurrence of ice clouds in the temperature range of -15°C to -20°C was also observed by previous studies (e.g., Wallace and Hobbs, 1977; Moss and Johnson, 1994)."

15. It is worth indicating sampling statistics (cloud length) for each cloud type in Table 1.

We revised Table 1 by adding these number of samples as recommended by the reviewer.

Table 1. Definitions of four transition phases of mixed-phase clouds, alongside their required spatial ratios of LCR, ICR, and MCR.

Phase	Description	Number of seconds	Number of TCRs	Spatial Ratio of LCR	Spatial Ratio of ICR	Spatial Ratio of MCR
				M1 = length of LCR / total segment length	M2 = length of ICR / total segment length	M3 = length of MCR / total segment length
1	Only LCR	8243	1163	M1 = 1	M2 = 0	M3 = 0

2	MCR appears	12557 (LCR: 11096, MCR: 1461)	142	$0 < M1 < 1$	$M2 = 0$	$0 < M3 \leq 1$
3	Pure ICR must appear	11988 (LCR: 3478, MCR: 2973, ICR: 5537)	249	$0 \leq M1 < 1$	$0 < M2 < 1$	$0 \leq M3 < 1$
4	Only ICR	8646	1193	$M1 = 0$	$M2 = 1$	$M3 = 0$

Concluding remarks

Given the amount of work invested in this study, I would encourage the authors to rewrite the paper accounting the above comments. I did not consider any minor comments since they are eclipsed by the major issues of this work. My biggest concern is related to the data quality issues. Fixing other issues is just a matter of time.

Alexei Korolev

We added all the new citations recommended by the reviewer into the main text.

Avramov, A., et al. (2011), Toward ice formation closure in Arctic mixed-phase boundary layer clouds during ISDAC, J. Geophys. Res., 116, D00T08, doi:10.1029/2011JD015910.

Baumgardner, D., and Coauthors, 2017: Cloud ice properties: In situ measurement challenges. Ice Formation and Evolution in Clouds and Precipitation: Measurement and Modeling Challenges, Meteor. Monogr., No. 58, Amer. Meteor. Soc., doi:10.1175/AMSMONOGRAPHS-D-16-0011.1.5

Fan, J., M. Ovtchinnikov, J. M. Comstock, S. A. McFarlane, and A. Khain, 2009: Ice formation in Arctic mixed-phase clouds: Insights from a 3-D cloud-resolving model with size-resolved aerosol and cloud microphysics. J. Geophys. Res., 114, D04205, doi:10.1029/2008JD010782.

Fan, J., S. Ghan, M. Ovchinnikov, X. Liu, P. J. Rasch, and A. Korolev, 2011: Representation of Arctic mixed-phase clouds and the Wegener-Bergeron-Findeisen process in climate models: Perspectives from a cloud-resolving study, J. Geophys. Res., 116, D00T07, doi:10.1029/2010JD015375

Field, P. R., R. J. Hogan, P. R. A. Brown, A. J. Illingworth, T. W. Choularton, P. H. Kaye, E. Hirst, and R. Greenaway, 2004: Simultaneous radar and aircraft observations of mixed-phase cloud at the 100 mscale. Quart. J. Roy. Meteor. Soc., 130, 1877–1904, doi:10.1256/qj.03.102

Field, P. R., A. A. Hill, K. Furtado, and A. Korolev, 2014: Mixed-phase clouds in a turbulent environment. Part 2: Analytic treatment. Quart. J. Roy. Meteor. Soc., 140, 870–880. doi:10.1002/qj.2175.
Hobbs, P.V., and A. L. Rangno, 1985: Ice Particle Concentrations in Clouds. J. Atmos. Sci., 42, 2523-2549, DOI: https://doi.org/10.1175/1520-0469(1985)042<2523:IPCIC>2.0.CO;2

Hill, A. A., P. R. Field, K. Furtado, A. Korolev, and B. J. Shipway, 2014: Mixed-phase clouds in a turbulent environment. Part 1: Large-eddy simulation experiments. Quart. J. Roy. Meteor. Soc., 140, 855–869, doi:10.1002/qj.2177.

Hogan, R. J., P. R. Field, A. J. Illingworth, R. J. Cotton, and T. W. Choularton, 2002: Properties of embedded convection in warm-frontal mixed-phase cloud from aircraft and polarimetric radar. Quart. J. Roy. Meteor. Soc., 128, 451–476, doi:10.1256/003590002321042054.

Korolev, A. V., and I. P. Mazin, 2003: Supersaturation of water vapor in clouds. J. Atmos. Sci., 60, 2957–2974, doi:10.1175/1520-0469(2003)060,2957:SOWVIC.2.0.CO;2.

Korolev, A. V., and G. A. Isaac, 2006: Relative humidity in liquid, mixed phase and ice clouds. J. Atmos. Sci., 63, 2865–2880, doi:10.1175/JAS3784.1.

Korolev, A. V., and P. R. Field, 2008: The effect of dynamics on mixed-phase clouds: Theoretical considerations. J. Atmos. Sci., 65, 66–86, doi:10.1175/2007JAS2355.1.

Korolev, A.V., E. Emery, J. W. Strapp, S. G. Cober, and G. A. Isaac, 2013b: Quantification of the effects of shattering on airborne ice particle measurements. J. Atmos. Oceanic Technol., 30, 2527–2553, doi:10.1175/JTECH-D-13-00115.1.

Korolev, A., McFarquhar, G., Field, P. R., Franklin, C., Lawson, P., Wang, Z., et al. 2017:. Mixed-phase clouds: Progress and challenges. Meteorological Monographs, 58, 5.1–5.50. https://doi.org/10.1175/AMSMONOGRAPHS-D-17-0001.1

Korolev, A., & Milbrandt, J., 2022: How are mixed-phase clouds mixed? Geophysical Research Letters,49, e2022GL099578. https://doi.org/10.1029/2022GL0995786

Morrison H, de Boer G, Feingold G, Harrington J, Shupe MD, Sulia K. 2011: Resilience of persistent Arctic mixed-phase clouds. Nature Geosci. DOI:10.1038/ngeo1332.

Moss, S. J. and Johnson, D.W. 1994 Aircraft measurements to validate and improve numerical model parametrization of ice to water ratios in clouds. Atmos. Res., 34, 1–25

Pinto, J. O., 1998: Autumnal mixed-phase cloudy boundary layers in the Arctic. J. Atmos. Sci., 55, 2016–2037, doi:10.1175/1520-0469(1998)055,2016:AMPCBL.2.0.CO;2.

Rauber, R.M, Tokay A. 1991: An explanation for the existence of supercooled liquid water at the top of cold clouds. J. Atmos. Sci. 48: 1005–1023.

Smith, A.J, Larson V.E, Niu J, Kankiewicz J.A, Carey L.D. 2009: Processes that generate and deplete liquid water and snow in thin midlevel mixed-phase clouds. J. Geophys. Res. 114: D12203, DOI: 10.1029/2008JD011531

Wallace, J. M. and Hobbs, P. V. 1975 Atmospheric Science: An introductory survey. Academic Press, New York, USA

Westbrook, C. D., and A. J. Illingworth (2011), Evidence that ice forms primarily in supercooled liquid clouds at temperatures > −27°C, Geophys. Res. Lett., 38, L14808, doi:10.1029/2011GL048021.

Response to comments from Reviewer 3

AMT review 3 comments

The purpose of this study is to evaluate varying cloud properties during the evolution of mixed phase clouds (i.e., from the first appearance of ice within supercooled liquid clouds to their complete glaciation). It tests for this by determining the ratio of liquid, mixed, and ice phase samples within a continuous cloud sample. Some important findings are revealed by the analysis, such as the vertical air motion is much more variable at the first appearance of ice at temperatures less than -20°C compared with other parts of the evolution, suggesting dynamical factors may be a significant factor for ice initiation.

The research topic is very important, as there are still large uncertainties associated with the evolution of mixed phase properties; and the novel approach qualitatively determining the stage of macroscale mixed phase evolution could be valid for a statistical analysis as undertaken in the study (assuming that once ice occurs within a supercooled liquid cloud, it will tend towards complete glaciation). This stage classification is often combined with the spatial extent of mixed and ice phase samples (ice spatial ratio). Findings can vary from quite insightful and perhaps striking (e.g., similar rates of increase in ice water content within mixed phase samples and also ice phase samples with increasing ice spatial ratio), to rather speculative (e.g., a key step for the Wegener-Bergeron-Findeison process to occur is when pure ice segments are present).

We thank reviewer 3 for the helpful comments and below is our individual response.

We revised the original sentence about the Wegener-Bergeron-Findeisen (WBF) process mentioned by the reviewer: "As ice crystals grow into pure ice segments (i.e., ICR), liquid phase starts to rapidly transition into ice phase, suggesting that the formation and growth of ice particles become more significant when pure ice segment appears."

Aside from the analyses performed, there are major concerns associated with their methodology listed below:

1) Specific combinations of LCR, MCR, and ICR ratios may be rather ambiguous. For example, are we sure a phase 2 cloud segment with >97.5% MCR is still considered to be in the earlier stage of glaciation than a phase 3 cloud segment with <2.5% ICR and >97.5% LCR? There is the potential for extreme ambiguity in what part of the mixed phase evolution a cloud region is currently in based on the current framework.

We agree with the reviewer that the previous analysis using ice spatial ratio as the transition indicator for both phases 2 and 3 can lead to an ambiguity. Therefore, in the revised manuscript, we use the definition of "mixed spatial ratio" for analysis of phase 2, to distinguish from ice spatial ratio in phase 3. Mixed spatial ratio is defined as mixed-phase cloud region (MCR) length over total cloud region (TCR) length i.e., mixed spatial ratio = length of MCR / length of TCR, calculated for each consecutive TCR.

In the first version of the manuscript, ice spatial ratio (ISR) was defined as: ISR = (ice cloud region ICR length + MCR length) / TCR length, calculated for each consecutive TCR. In that previous definition, ICR and MCR carry the same weight when their spatial extent contributes to spatial fraction of ice-containing segments. We revised it to: ISR = (ICR length + MCR length * IWC/TWC) / TCR length, calculated for each consecutive TCR. In this revised definition, MCR's contribution to ice-containing segment spatial extent is reduced since its average ice mass fraction is less than 1.

All the figures are revised according to these new definitions of mixed spatial ratio and ice spatial ratio mentioned above. The new **Figure 7** is shown as an example using the revised mixed spatial ratio and ice spatial ratio below.

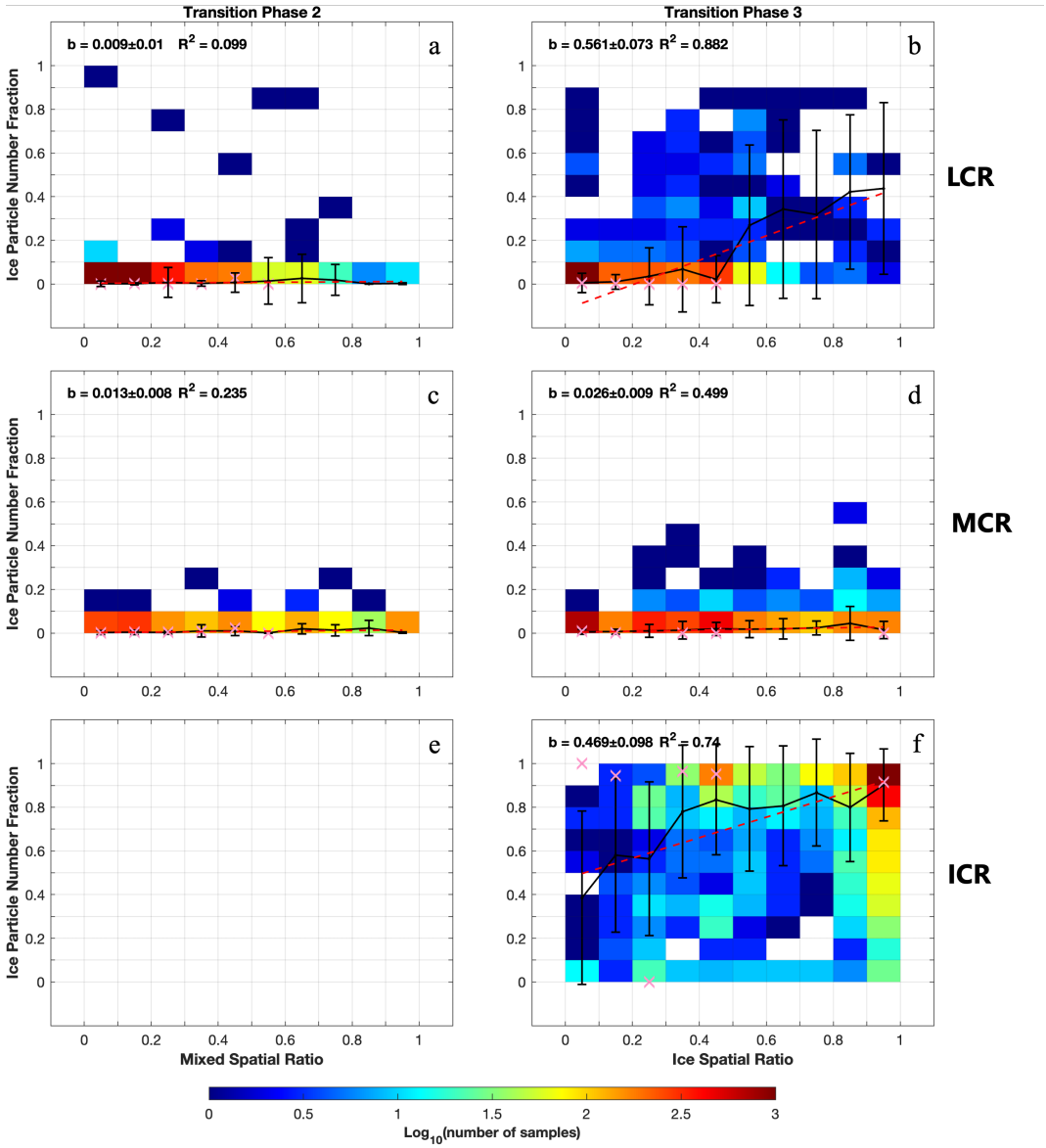

Figure 7. Relationship between ice particle number fraction and mixed spatial ratio or ice spatial ratio, separated by the transition phases (phase 2 in column 1 and phase 3 in column 2), and by various cloud segments – (a, b) LCR, (c, d) MCR and (e, f) ICR. Average values for each ice spatial ratio bin are shown in black solid lines, with vertical bars representing standard deviations. Linear fit is shown in red dashed line. Average values of generating cells (time series obtained from Wang et al. (2020)) are in pink "X" markers. The slope value b, its associated standard deviation, and the ordinary R-squared value are shown in the legend.

2) This study does not appear to account for whether the aircraft is sampling within the cloud or the precipitation underlying a given cloud. So a primarily liquid phase cloud (with few mixed phase samples) could be precipitating ice and if the aircraft samples the precipitation, it will be considered phase 3, although the cloud itself would be phase 2. Not to mention, the aircraft could have a majority of cloud samples/an entire length of continuous cloud sampling as precipitation. Including precipitation likely accounts for subsaturated conditions for both liquid and ice phase samples in Figures 10 and 11.

We agree with the reviewer that the previous analysis did not account for the potential precipitation underlying a given cloud. To identify these precipitating clouds, we analyzed two new airborne remote sensing instruments – the HIAPER Cloud Radar (HCR) and High Spectral Resolution Lidar (HSRL). We used the particle identification (PID) value added product provided by the NCAR Earth Observing Laboratory (EOL) team to identify and remove precipitating samples. The PID includes 11 types of conditions. We made time series figures for every hour of each research flight (RF) and zoomed into each segment to manually inspect possible precipitating samples.

We added the text in section 2.1: "To provide a more focused analysis of cloud layers instead of precipitation below the clouds, we use two remote sensing instruments onboard the G-V aircraft – NSF/NCAR High-performance Instrumented Airborne Platform for Environmental Research (HIAPER) Cloud Radar (HCR) and High Spectral Resolution Lidar (HSRL) to identify potential precipitating samples. The particle identification (PID) product is used, which includes identifications of 11 categories – rain, supercooled rain, drizzle, supercooled drizzle, cloud liquid, supercooled cloud liquid, melting, large frozen, small frozen, precipitation and cloud (Romatschke and Vivekanandan, 2022). By manually inspecting hourly time series of this product, we remove segments that are identified as precipitation, supercooled drizzle, drizzle, supercooled rain, and rain. In addition, we further examined the NSF SOCRATES campaign field catalogue for each flight to ensure that we do not miss any precipitation segments that have been identified in the field catalogue. The time stamps of the beginning and end of these segments are stored in supplemental Table S1. For most flights, we identified on average about 5 – 20 minutes of samples of precipitating regions, except RF15 which has about an hour of precipitating samples. It is worth noting that most of these segments occur at temperatures above 0°C, while this study only focuses on -40°C to 0°C."

Table S1. Time stamps of precipitating segments identified in the NSF SOCRATES campaign that are excluded from this study.

Research flight (RF)	Time stamps of precipitation segments removed
RF01	N/A
RF02	5:55 to 6:32 UTC
RF03	23:50 to 00:00 UTC, 00:00 to 00:05 UTC, 00:34 to 00:40 UTC, and 01:16 to 01:32 UTC
RF04	03:47 to 03:52 UTC
RF05	04:40 to 05:00 UTC
RF06	02:28 to 02:32 UTC
RF07	05:10 to 05:15 UTC
RF08	05:00 to 05:10 UTC
RF09	04:29 to 04:32 UTC
RF10	02:44 to 02:56 UTC, and 03:58 to 04:00 UTC
RF11	03:41 to 03:46 UTC
RF12	05:09 to 05:15 UTC
RF13	03:40 to 03:50 UTC, and 04:38 to 04:43 UTC
RF14	03:19 to 03:28 UTC, and 04:38 to 04:42 UTC
RF15	07:20 to 08:36 UTC

Minor concern:

1) The lengths of the clouds used in the mixed phase evolution appear (note: the lengths are not clearly defined in the text) to not be set to a constant length, so some lengths could vary from two or three cloud samples (are single 1 Hz cloud samples without neighboring cloud samples removed?) to hundreds of

samples. This means processes associated with different length scales will have different impacts on different cloud lengths and may not result in an apples-to-apples comparison.

This is a very good point. In fact, in the beginning stage of our analysis, we tested two ways of analyzing these segments. One way is to average each TCR cloud segment into a single datum point. But we decided to choose the other way for this analysis, which keeps each second of a segment as a separate sample, that way if a shorter segment only has a few seconds while a longer segment has hundreds of seconds, the longer segment will carry a higher weight since it will provide more 1-Hz samples for the final analysis. The latter method reflects the radiative impacts in the real atmosphere better, since clouds with larger spatial extent also have larger radiative effects. We added a supplemental Figure S1 to illustrate this method more clearly.

With that said, we agree that the length of the segment needs to be clarified in the manuscript better. We also would like to clarify regarding the reviewer's concern about "*are single 1 Hz cloud samples without neighboring cloud samples removed*". This indeed has been discussed in our team in the method development stage, but we didn't mention this detailed filtering process in our first manuscript, and now we added this process in the section 3.1: "In the second step, a total cloud region (TCR) that can potentially contain a combination of LCR, ICR and MCR is identified, which basically is a consecutive in-cloud segment surrounded by clear-sky conditions. If a TCR sample is surrounded by two adjacent seconds of NaN, then this sample is deleted, because one cannot determine if the NaN points are the edge of the cloud or if they are still part of the cloud. But if a TCR sample is surrounded by two adjacent seconds of clear-sky samples, then this in-cloud sample is valid, and its measurement can last from one second to many seconds. For instance, if five seconds of LCR are adjacent to one second of MCR, then both the LCR and MCR belong to the same TCR. An illustration of the identification of TCR is shown in supplemental Figure S1. All the 1-Hz samples within the TCR are used in the analysis in the following sections. The length of each second of sample within an TCR is calculated based on the aircraft true air speed at that specific second. The length of each TCR is calculated as the sum of all in-cloud samples within that TCR. The mean true air speed of the G-V research aircraft between -40°C and 0°C during the SOCRATES campaign is ~172 m/s."

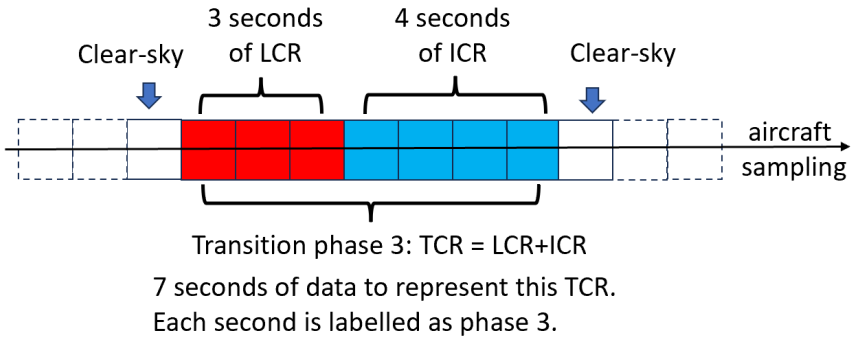

Figure S1. A schematic diagram that illustrates the identification of a total cloud region (TCR) sample, with liquid cloud region (LCR) and ice cloud region (ICR) embedded inside this TCR. All 7 seconds of samples inside this TCR are used in the analysis of cloud properties.

I think a good start for addressing these issues is to take a good look at the individual total cloud regions: the distribution of their lengths as well as their phase ratios and how they look for the individual "phases of mixed phase evolution."

As we clarified above, this work indeed examines individual, consecutive TCR and calculates the mixed spatial ratio or ice spatial ratio for each TCR. The distributions of the TCR lengths are added as two sub-

panels in **Figure 3,** which illustrates the number of samples and the frequency distributions of TCR lengths for 4 transition phases. The number of samples of the ice spatial ratios of individual TCRs is illustrated in new Figure 7 (shown in our response on a previous page), which shows the relationship between ice number particle fraction and mixed (or ice) spatial ratio.

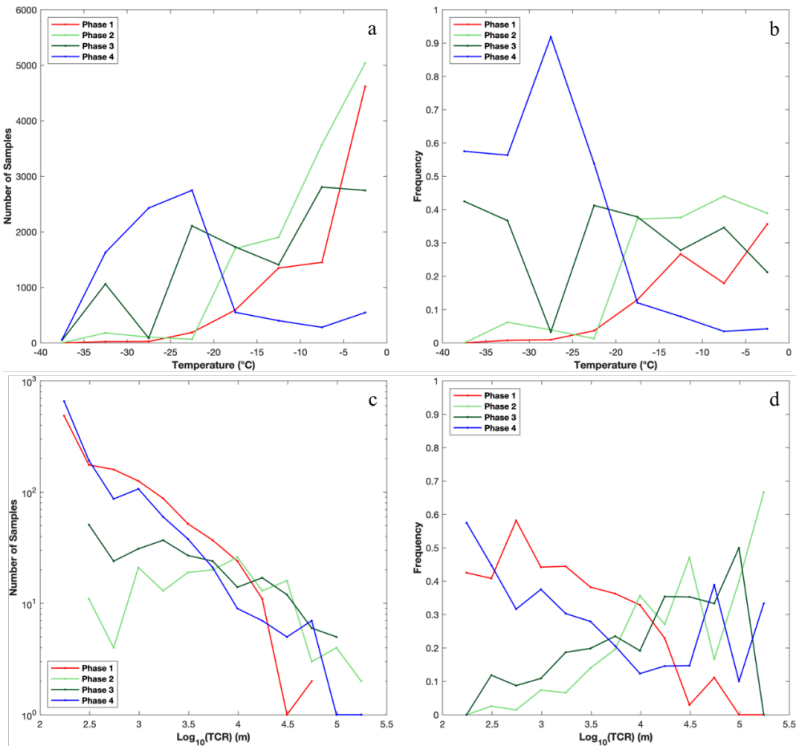

Figure 3. Distributions of four transition phases at various temperatures in terms of (a) number of 1-Hz samples and (b) frequency of each phase. In (b), the frequency of each phase is normalized by the number of samples of all phases in each 5-degree temperature bin. (c) Number of 1-Hz samples and (d) frequency distribution of TCR lengths in logarithmic scale. In (d), frequency is calculated as the number of 1-Hz samples of a specific phase divided by the total number of 1-Hz in-cloud samples in each $10^{0.25}$ bin.

There are also other major concerns aside from the mixed phase evolution methodology:

1) The authors use the UHSAS probe to discern aerosol concentrations within the clouds. However, it appears as though aerosol measurements are taken within the cloud samples. This is problematic as there is a high likelihood the probe is sampling the residuals of cloud particles, and I suspect the positive correlation of aerosols with diameters greater than 500 nm within greater ICR is the UHSAS sampling cloud particle residuals. In order to use the UHSAS in the cloud, it is vital to provide sensitivity tests to confirm no such biases are occurring for both liquid and ice particles.

We thank the reviewer for pointing out this potential issue. To address this issue, we first examined segments by segments of in-cloud samples of concurrent measurements of UHSAS probe and cloud probes, and we did not see any evidence of cloud hydrometeor mass or number concentrations correlated with aerosol number concentrations at 1-Hz resolution. In addition to this inspection, we revised **Figure 10** by applying a moving average on aerosol number concentrations for every 50 seconds, which is about 10-km resolution. We also tested the results when using the 100-second moving averages of aerosol number concentrations (**supplemental Figure S10**), which is about 20-km resolution. The relationships

between average aerosol number concentrations for diameters greater than 500 nm and 100 nm (i.e., $N_{>500}$ and $N_{>100}$, respectively) and cloud microphysical properties (i.e., LWC, IWC, Nliq, and Nice) are examined. Similar aerosol indirect effects on ice and liquid are shown in these new analyses compared with our previous analyses in the original manuscript. We added the comments in section 3.5: "Due to the possible complication of in-cloud measurements of aerosol number concentrations, we applied a moving average to calculate logarithmic scales of aerosol concentrations at every 50 seconds in Figure 10. A coarser spatial averaging using the 100-second moving average is also shown in supplementary Figure S10."

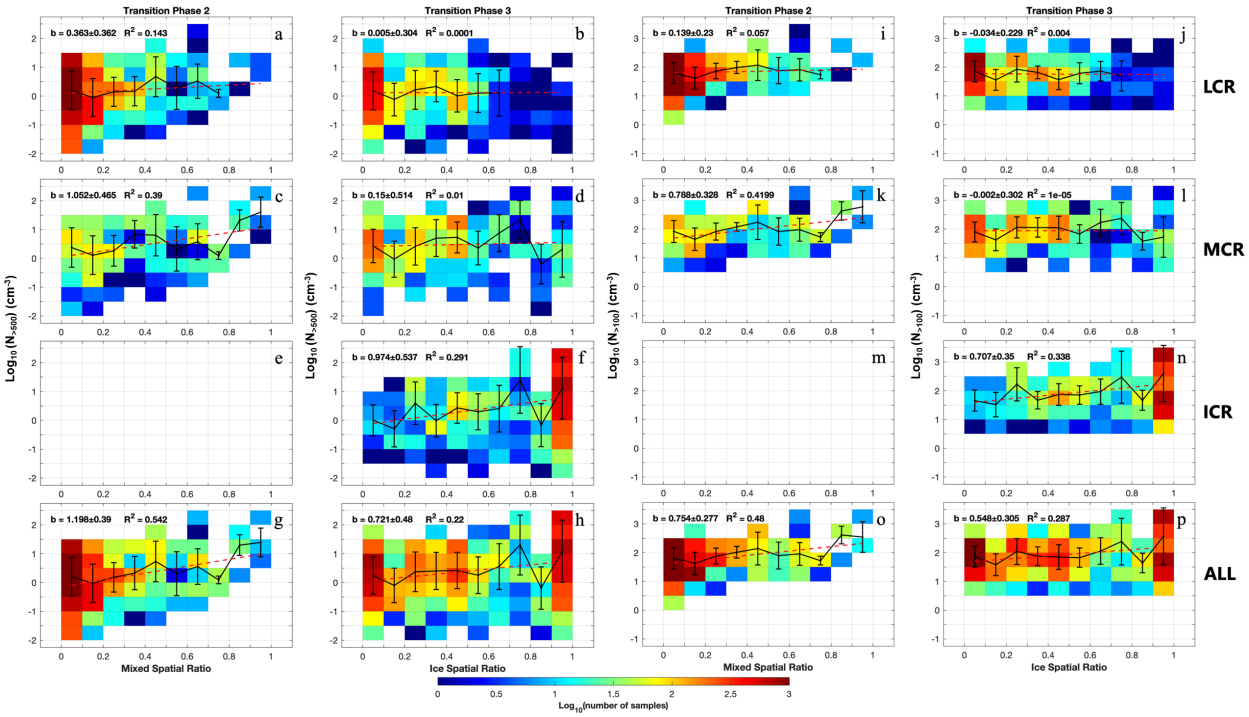

Figure 10. Similar to Figure 7, but showing logarithmic scale (a-h) $N_{>500}$ and (i-p) $N_{>100}$ in relation to mixed spatial ratio or ice spatial ratio, separated by the transition phases and cloud regions. The last row represents all cloud regions in a specific transition phase. The aerosol number concentrations represent the moving average values of every 50 seconds.

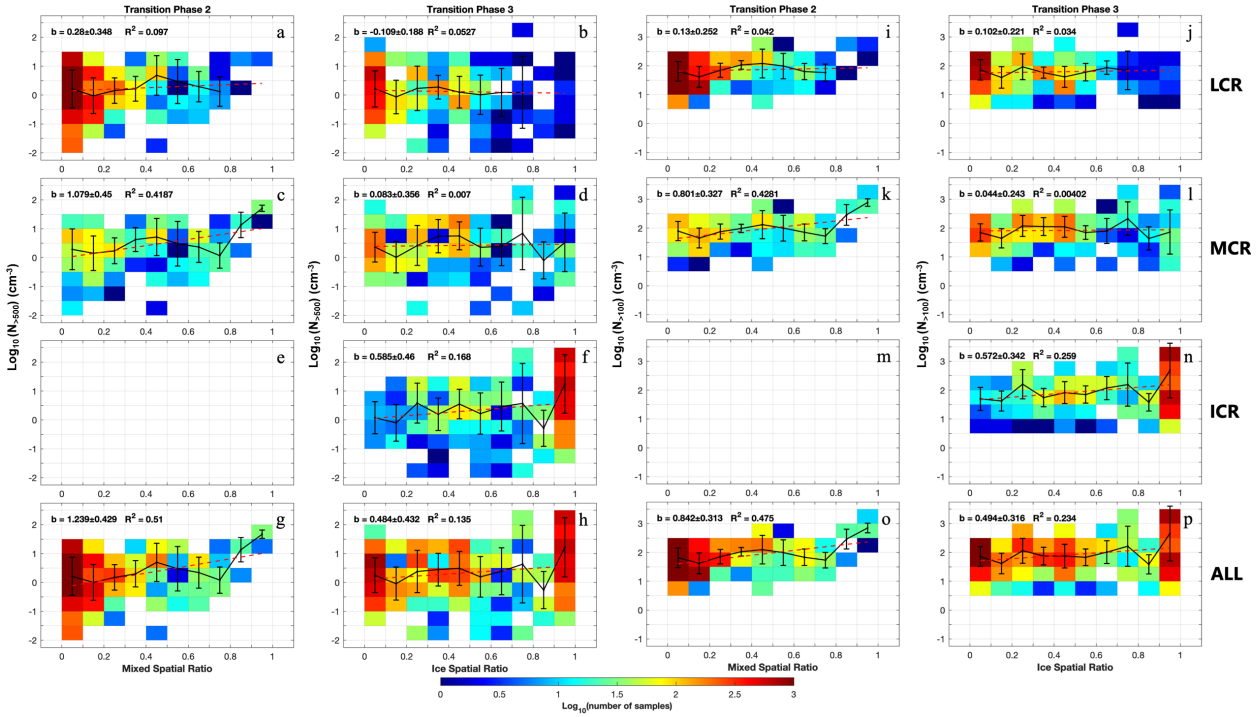

Figure S10. Similar to Figure 10 in the main manuscript but using 100-second moving averages of logarithmic scales of $N_{>500}$ and $N_{>100}$. The results using the coarser scale of aerosol number concentrations are very similar to those shown in Figure 10.

2) Phase frequencies are determined using a phase definition relating the phase fraction of liquid to the total number of particles using the UWLID product. However, it was stated that the 2DS has a size range of 40-5000um. Assuming the UWLID product provides phase information for this particle size range (does it? If so, the smaller particle sizes [<~200 um] should be associated with large uncertainties due to the loss of the 2DS imaging resolution), what about particles less than 40 um? It doesn't seem like the CDP measurements are incorporated into the analysis, which could significantly impact number concentration ratios.

We thank the reviewer for catching this error. That is correct, we previously did not add the CDP measurements into the number of liquid droplets for this calculation. In the revised manuscript, we calculated the number concentrations of both liquid droplets and ice particles from 2DS, then added the liquid droplet number concentration together with the CDP liquid droplet number concentrations. This new calculation affects new **Figures 7 and 9** which both contain the ice particle number fraction analysis. We clarified this calculation in section 2.2: "We use the hydrometeor count defined by the maximum diameter in the UWILD dataset to calculate Nliq and Nice detected by the 2DS probe within each second. Then we further add Nliq detected by CDP to those detected by 2DS to derive the total Nliq. Finally, we define ice particle number fraction, which equals Nice / (Nice + Nliq) in one second."

There were quite a few grammatical errors as well, and multiple citations were in error. And although there are some interesting findings presented in this study, I unfortunately cannot recommend that this manuscript be accepted for publication. I recommend doing a thorough revision of the paper and resubmitting.

We appreciate the reviewer for the comments. We have conducted a more thorough proofreading of the text, corrected the grammatical errors and revised the reference list.